THE UNIVERSITY OF ALBERTA

THE DESIGN AND CONSTRUCTION OF AN OUTDOOR ICING WIND TUNNEL, AND SOME PRELIMINARY SEA-SPRAY ICING EXPERIMENTS

by

Aleksander Nowak

A THESIS

SUBMITTED TO THE FACULTY OF GRADUATE STUDIES AND RESEARCH

IN PARTIAL FULFILMENT OF THE REQUIREMENTS FOR THE DEGREE

OF Master of Science

IN

Meteorology

Geography

EDMONTON, ALBERTA

Spring 1988

Permission has been granted to the National Library of Canada to microfilm this thesis and to lend or sell copies of the film.

The author (copyright owner) has reserved other publication rights, and neither the thesis nor extensive extracts from it may be printed or otherwise reproduced without his/her written permission.

L'autorisation a été accordée à la Bibliothèque nationale du Canada de microfilmer cette thèse et de prêter ou de vendre des exemplaires du film.

L'auteur (titulaire du droit d'auteur) se réserve les autres droits de publication; ni la thèse ni de longs extraits de celle-ci ne doivent être imprimés ou autrement reproduits sans son autorisation écrite.

ISBN 0-315-42731-0

THE UNIVERSITY OF ALBERTA

RELEASE FORM

NAME OF AUTHOR Aleksander Nowak

TITLE OF THESIS THE DESIGN AND CONSTRUCTION OF AN OUTDOOR ICING WIND TUNNEL, AND SOME PRELIMINARY SEA-SPRAY ICING EXPERIMENTS.

DEGREE FOR WHICH THESIS WAS PRESENTED Master of Science

YEAR THIS DEGREE GRANTED Spring 1988

Permission is hereby granted to THE UNIVERSITY OF ALBERTA LIBRARY to reproduce single copies of this thesis and to lend or sell such copies for private, scholarly or scientific research purposes only.

The author reserves other publication rights, and neither the thesis nor extensive extracts from it may be printed or otherwise reproduced without the author's written permission.

(SIGNED) .....

PERMANENT ADDRESS:

ul.: A. Krzywoń 27

31 464 Kraków

Poland

DATED 31 December 1987

THE UNIVERSITY OF ALBERTA

FACULTY OF GRADUATE STUDIES AND RESEARCH

The undersigned certify that they have read, and recommend to the Faculty of Graduate Studies and Research, for acceptance, a thesis entitled The Design and Construction of an Outdoor Icing Wind Tunnel, and Some Preliminary Sea Spray Icing Experiments submitted by Aleksander Nowak in partial fulfilment of the requirements for the degree of Master of Science in Meteorology.

Edward J. Bowen

Supervisor

R. Charlton

A. H. Lak

Date 21 December 1987

ABSTRACT.

A small, single loop, outdoor icing wind tunnel has been designed and built. Procedures for untertaking sea-spray icing experiments in this tunnel have been developed. A limited number of sea-spray and fresh water spray experiments were carried out during the winter of 1984-1985.

The range of temperatures tested was between -6.2°C and -12.6°C. Two wind speeds, 10 m/s and 15 m/s were used. The icing model, a hollowed aluminum cylinder .0254 m in diameter, was not rotated. The liquid water content was either 5 g/m³, or 7.7 g/m³. The median volume diameter of the droplets was 150 micrometers.

The experimental results showed that there was a significant difference between salty water accretions and fresh water accretions. The salty accretions were heavier, spongier, milkier in appearance, more fragile and asymmetric than the fresh water accretions.

The results of a simple numerical model were compared to the experiments. Numerical simulations were performed for the same conditions as during the icing experiments. The model underestimated the rate of accretion in both the fresh water and the salty water cases.

ACKNOWLEDGEMENT

I would like to express my sincere thanks to Dr. E.P. Lozowski for his continuing support, encouragement and advice. His help and patience is very much appreciated.
I would also like to thank Dr. E.M. Gates of the Department of Mechanical Engineering without whom the tunnel could not have been built.

Thanks to Mr. Tom Villet and his staff in the Mechanical Engineering Workshop who put the tunnel together. Thanks to the other students of the icing research team whose advice, inspiration and constructive criticiszm were most helpful.

Last, but not least, thanks to my mother-in-low Anna Kozlowski whose persuasion and sustenance helped to finalize this work.

Table of Contents

Chapter		Page
1.	INTRODUCTION	1
2.	CHARACTERISTICS OF MARINE ICING.	5
	2.1 Spray generation processes.	7
	2.1.1 Wind-generated spray.	8
	2.1.2 Wave-generated spray.	11
	2.1.3 Total spray flux.	15
	2.2 Conditions for spray icing.	15
3.	THE PHYSICS OF ICE ACCRETION.	20
	3.1 Droplet - object interaction.	20
	3.2 Droplets in flight.	29
	3.3 The heat balance of an accreting surface.	30
	3.4 Solution of the heat balance equation.	37
4.	DESIGN, CONSTRUCTION AND CALIBRATION OF THE ICING WIND TUNNEL.	40
	4.1 Tunnel design.	40
	4.2 Spraying system.	45
	4.3 Temperature measurement.	46
	4.4 Air speed measurement.	46
	4.5 Liquid-water content measurement.	47
	4.6 Droplet size distribution measurement.	48
5.	PROCEDURES AND EXPERIMENTS.	50
	5.1 Procedures	51
	5.2 Experiments.	52
6.	RESULTS AND DISCUSSION.	57
	6.1 Effect of cylinder orientation.	57
	6.2 Effect of varying the liquid water content.	58
	6.3 Effect of varying wind speed.	59

6.4 Effect of air temperature. 59

6.5 Differences in accretion appearance. 59

6.6 Comparison between the experimental results and the numerical simulations. 64

7. SUMMARY, CONCLUSIONS AND SUGGESTIONS FOR FUTURE STUDY. 68

BIBLIOGRAPHY. 71

APPENDIX A1 75

APPENDIX A2 76

1. INTRODUCTION

Severe weather conditions in cold maritime regions require special research and engineering efforts. Ice storms have been the cause of many dangerous situations, which have often resulted in substantial damage and casualties. Numerous vessels and their crews have been lost due to ice accretion (Minsk, 1977; Stallabrass, 1979), especially during the last three decades, since human activities in polar and subpolar regions have been intensified. The developement of off-shore oil resources has resulted in an increasing interest in marine icing. Although icing on semi-submersible drilling vessels does not seriously affect their stability, it may cause a major inconvenience in maintaining activities on them (eg.:slippery walkways, iced instrumentation, or the hazard of falling ice). Marine icing may also affect helicopters and small boats used to carry personnel and supplies between the rigs and the shore.

A number of scientists have been investigating marine icing. Icing on fishing vessels has been identified as a significant hazard by Stallabras(1971,1979,1980) and Minsk(1980). The meteorological aspects of ice accretion on ships have been surveyed by Shellard(1974) and Jessup(1985). An attempt to simulate the process of marine icing has been made by Katchurin(1974), Stallabrass(1979), Makkonen & Stallabrass(1984) and Horjen(1984). The papers of Itagaki(1984), Minsk(1980), Makkonen(1984) and Gates & Lozowski(1985) all point out that, even though this problem

has been around for some time, it has yet to be solved. Icing conditions at sea, characterized by a relatively high liquid-water content, large droplet size and temperatures close to the freezing point, are very complex. Stallabrass(1971) listed the five following causes of ship icing:

1. Supercooled fog(Arctic sea smoke);
2. Freezing rain or drizzle;
3. Falling snow (particularly wet snow);
4. Wind generated sea spray(spindrift);
5. And the most serious, sea spray generated by the passage of a vessel through heavy seas, when the temperatures of air and sea are low.

Very often, a combination of some or all of the above conditions exists, making the icing problem even more complex. Borisenkov and Panov(1972), using the statistical analysis of more than 2000 cases of icing on fishing vessels, showed that the most frequent cause was sea-water spray alone(50% for Arctic seas and 89.8% for the remaining northern waters). Thus, there is clearly a need for a detailed investigation of sea spray icing conditions and causes.

Experimentation on shipboard icing is an enormous task in itself, since in any particular experiment one can handle only a few parameters of limited range. Also, this type of experiment is very costly, and it may be hazardous. Some scientist(Stallabrass, 1971) have made attempts simply to

map the dangerous regions where heavy icing may occur. However, if avoidance is the solution, this would eliminate vast areas of endangered waters from any activity sensitive to icing for the winter season.

Since the problem of sea-water spray icing is very complex, it is necessary to use all available research tools, including wind tunnel experiments. There are very few research facilities around the world, in which this problem can be studied in a controlled way. Although many atmospheric icing wind tunnels are now operational (Lozowski & Gates, 1985), they are not suitable for studying sea water spray icing, because of the corrosive effects of sea water, and also because of the inability to produce the required droplet sizes. As far as is known, there were no marine icing tunnels available in Canada at the time of the experiments described in this thesis. The only marine icing tunnels known were located at the Institute of Marine Research in Helsinki Finland, and at the Norwegian Hydrodynamic Laboratory in Trondheim.

The purpose of this thesis was to conduct sea-water spray icing experiments in realistically simulated natural conditions. The work concentrates on those aspects of marine icing which are considered to be most crucial. This includes studies of the dependence of icing upon temperature, aerodynamic conditions and liquid water content. Special attention is given to a comparison between the regimes of sea water spray icing and fresh water spray icing.

Since the use of salty water is not allowed in the existing wind tunnels at The University of Alberta, the first step was the design and construction of a completely new wind tunnel. It is a small, unrefrigerated, open loop wind tunnel capable of simulating sea water spray icing conditions. The background theory for this work is outlined in Chapter 2 and 3. The design and construction of the tunnel is described in Chapter 4. The experiments and experimental procedures are described and documented in Chapter 5. Chapter 6 discusses the results, and the possible implications for sea spray icing. Chapter 7 summarizes the study and gives suggestions for future research.

2. CHARACTERISTICS OF MARINE ICING.

Although atmospheric icing has been studied quite extensively, and is fairly well understood, the results are difficult to transpose to marine icing conditions. Marine icing differs from fresh water accretion in a number of ways. Whereas atmospheric icing usually occurs in cloud or fog with very small droplets, marine ice accretion is the result of sea-spray with much larger droplet sizes(see Table 2.1). Volume median diameters in icing clouds are typically anywhere from about 10 to 20 micrometers, but sea spray may involve droplets of up to several millimeters in diameter. Due to their small sizes and long residence times, droplets in clouds are usually very close to the air temperature. Marine spray, however, will achieve a temperature somewhere between the ocean surface temperature and that of the air. Atmospheric ice accretion usually consists of rime ice, in which the impinging droplets immediately freeze as spheres where they hit the icing object. In marine icing conditions, with larger droplet sizes, higher liquid water contents and a lower degree of supercooling, the droplets may not freeze entirely on impact, but the unfrozen water will usually run along the surface of the icing object and freeze where the heat transfer is higher. The spray will also impact intermittently, complicating the heat transfer conditions even more.

Table 2.1 Characteristic of icing sources in the atmospheric surface layer. (From Makkonen, 1984)

Source	Droplet diameter (μm) Range	Mean	Liquid water content ($g\ m^{-3}$)	Reference
Sea spray on a moving ship	1000 - 3500	2400	0 - 219	Borisenkov and Panov (1974)
Sea spray in first 10 cm	10 - 1000	200	--	Wu (1979)
Sea spray on a stationary ship				
$v > 15\ m\ s^{-1}$, $h = 2\ m$	3 - 2000	5 - 30	0.03	Preobrazhenskii (1973)
$v > 15\ m\ s^{-1}$, $h = 7\ m$	3 - 90	5 - 30	0.00	Preobrazhenskii (1973)
Marine advection fog	--	8 - 16	0.03 - 0.17	Fitzgerald (1978)
Coastal fog	4 - 20	--	0.01 - 0.16	Goodman (1977)
Evaporation fog	6 - 120	13 - 38*	0.01 - 0.30	Houghton and Radford (1938)
Evaporation fog	--	--	0.04 - 0.14	Bashkirova and Krasikov (1958)
Evaporation fog	--	8 - 10	0.20	Currier et al. (1974)
Arctic fog	7 - 130	16	0.00 - 0.15	Kumai (1973)
Arctic fog	2 - 75	18	0.02	Kumai and Francis (1962)
Arctic fog	6 - 60	--	0.04 - 0.17	Reiquam and Diamond (1959)
Continental winter fog	--	10	0.00 - 0.45	Pinnick et al. (1978)
Mountain fog	--	7 - 23*	0.05 - 0.30	Bain and Gayet (1982)
Low stratus	2 - 43	5	0.05 - 0.25	Pilie and Kocmond (1967)

*Median-volume diameter.

The process of spray generation, and consequently the vertical distribution of droplet size and liquid water content, is difficult to quantify, especially given the intermittent and irregular nature of this process. Another major difference between freshwater and marine icing is expected to be the effect of salinity on the ice accretion. The resulting depression of the freezing point, and the incorporation of brine pockets into the accretion, will almost certainly lead to differences in ice accretions grown in otherwise similar conditions. Like spray, not enough is known about wind in the marine boundary layer, even though it is the major driving force for icing and spray generation.

2.1 Spray generation processes.

Since icing from freezing spray is the most common cause of vessel icing, special attention has to be paid to the process of sea-spray generation. In an effort to derive the icing rates of ships as a function of water delivery, Zakrzewski(1986) has investigated the action of the wind on the waves (wind-generated spray), and the action of the ships themselves on the waves (ship-generated spray). These are the two processes responsible for sea spray generation.

2.1.1 Wind-generated spray.

Two mechanisms are responsible for wind-generated spray production:

- direct whipping of wave crests by the wind;
- bursting of entrained air bubbles at the water surface, after the wave collapses.

The second mechanism is thought to be the primary source of wind generated spray.

The least known and yet most important parameter is the vertical distribution of liquid water content(*LWC*) in wind-generated spray. Some experimental data are available to estimate the vertical distribution. In general, the vertical characteristic of sea spray *LWC* depends on wind speed and wave height. This dependence is not simple, because the wind speed affects not only *LWC*, but also the wave height. Moreover, the wave height also depends on the duration of the wind and the fetch. Preobrazhenskii(1973) has proposed the followimg formula for the vertical distribution of *LWC*:

$$LWC = w_o \exp(-\beta(z-\frac{H}{2})) \quad [kgm^{-3}] \qquad (2.1.1.1)$$

where z is the height above mean water level, H is the wave height, and w_o and β are constants, derived empirically for various wind speeds. Zakrzewski(1986) has gone further,

investigating the relationships between *LWC* and various other parameters. According to Zakrzewski(1986), a number of spray generation regimes can be distinguished depending on the state of the sea. He gave a set of constants for Equation 2.1.1.1 depending on wave height and wind speed, with a wind speed of 5 m/s being the threshold value for spray production. Empirical equations for *LWC* distribution in sea spray, given in Zakrzewski's paper, are quite easy to apply, if one has reliable wave height and wind speed estimates. The assumption used by Zakrzewski is that the wind profiles are logarithmic in the so called "Prandtl layer." This assumption holds only in neutral atmospheric conditions. During an icing event, the air over the sea is always unstable, and in order to estimate the wind profiles in the lowest layer, turbulent momentum transfer has to be considered.

The shortest way to determine the characteristics of wind generated spray, is to use charts constructed from experimental data (see Figure 2.1.1.1). A number of such charts are shown in Zakrzewski's paper(1986). However, one should be aware that none of these charts is fully representative of all sea conditions. They are site and ship specific, and they do not cover the whole spectrum of possible meteorological conditions as they are constructed from a limited number observations collected at random.

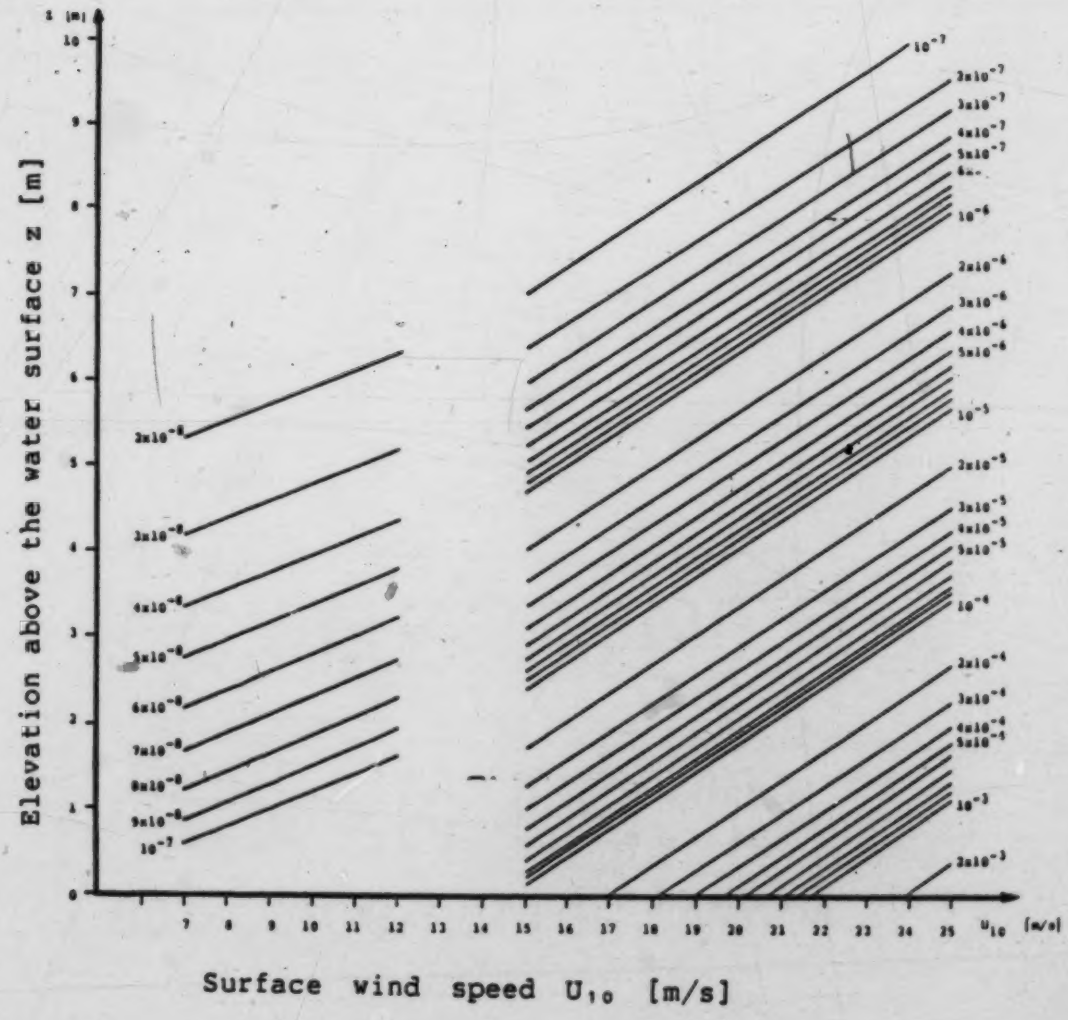

FIGURE 2.1.1.1 Liquid water content in wind-generated spray as a function of surface wind speed (from Zakrzewski, 1986).

2.1.2 Wave-generated spray.

Wave-generated spray is produced by ship-wave interaction. A cloud of spray, produced by wave impact on a ship, becomes wind rafted and splashes onto the ship. The water flux delivered to the ship in the form of spray, depends on the ship's relative motions with respect to wave motion and wind speed, and also on wave height and wave period. Zakrzewski(1986) approached this problem by examining a single wave impact on a ship and the frequency of generation of the spray cloud. The liquid water content in a wave-generated spray cloud is rather poorly known, mainly due to very scarce data. Katchurin(1974) proposed that *LWC* is a function of wave height only:

$$LWC = \zeta \cdot H \quad [kgm^{-3}] \qquad (2.1.2.1)$$

where H is the wave height and ζ is a constant. This equation is valid only for ships moving into the waves with a heading of 140°-180°. Zakrzewski(1987, private communication) has suggested that the LWC distribution above the ship's deck should be proportional to the wave height, and to the square of the ship's speed relative to the surface of an oncoming wave. He recommends the following formula for LWC:

$$LWC = 6.1457 \cdot 10^{-5} H \cdot V_o^2 \cdot \exp(-0.55h') \quad [kgm^{-3}] \qquad (2.1.2.2)$$

where H is the wave height, h' is the elevation above the ship's deck, and V_o is the ship speed relative to the wave movement. From Equation 2.1.2.2 one may see that:

1. LWC decreases with increasing height above the ship's deck;
2. LWC increases with increasing wind speed;
3. LWC is maximal for ships moving into the waves and minimal for ships moving with the waves;
4. LWC increases as the ship's speed into the waves increases;
5. LWC does not depend on the ship's speed for ships moving parallel to the waves.

Zakrzewski (1986) has carried out a quantitive analysis of the above relationships, and has given them in the form of nomograms which are useful for estimating realistic sea-spray icing conditions. One of these nomograms is shown in Figure 2.1.2.1.

In order to determine the time-averaged water flux to any place on a ship, the time of the ship's exposure to the spray from a single wave impact and the frequency of the impacts also have to be known. As the morphology of the spray cloud is generally unknown, only a rough approximation of that time can be made. Zakrzewski (1986) gives the following formula:

$$\Delta t = c \frac{HV_o}{U^2} \qquad (2.1.2.4)$$

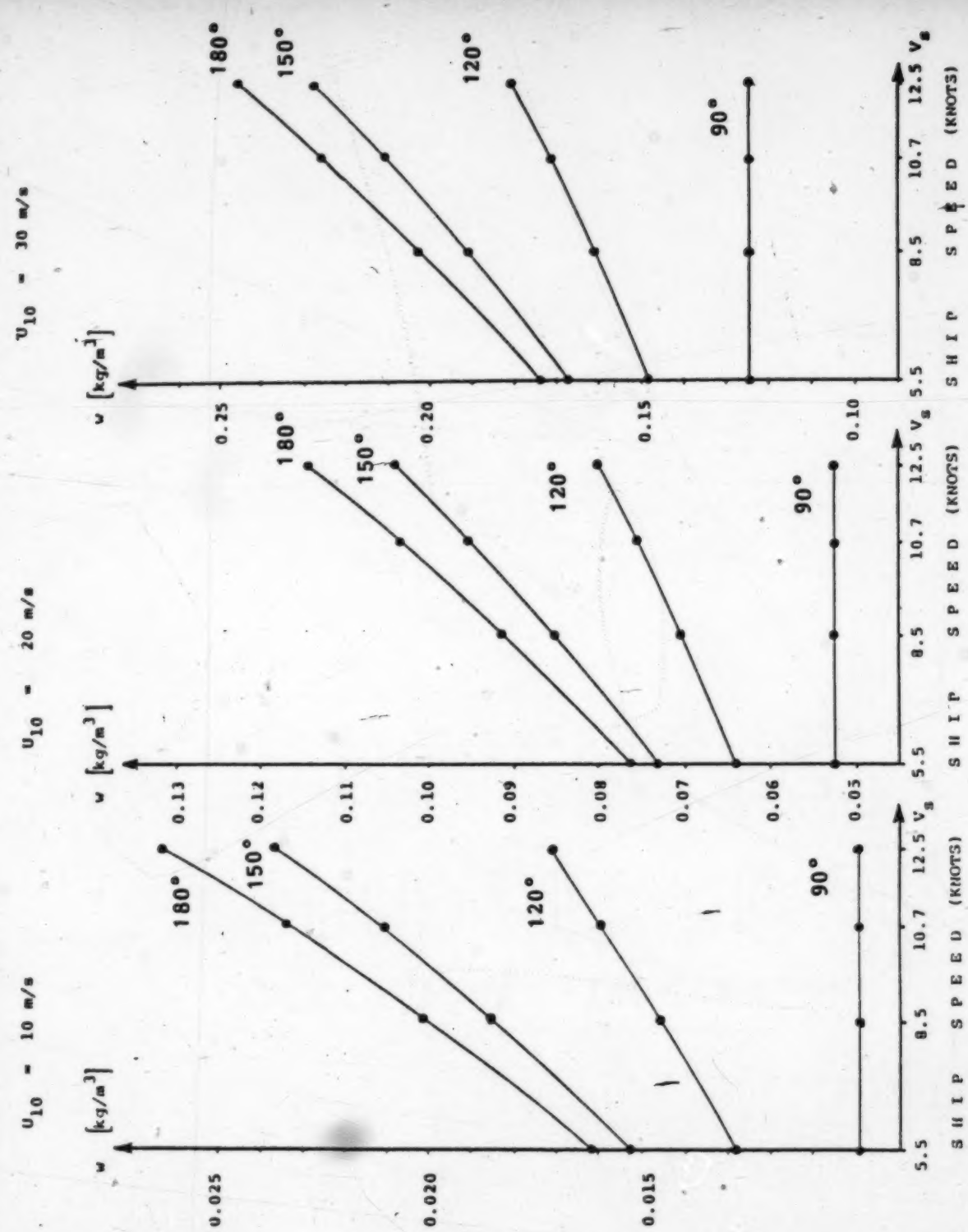

Figure 2.1.2.1 Liquid water content in wave generated spray as a function of ship speed and heading angle for an elevation of 1 m above the ship's deck (from Zakrzewski, 1986).

where C is an empirical constant which depends mainly on the ship's architecture. The impact frequency is not simply determined by the wave frequency. Zakrzewski(1986), analysing available analytical expressions for wave impact frequencies, and frequencies observed by others, concluded that on average, a ship is splashed by every second wave. Panov's(1971) formula for the frequency of the splashes seems to be the most appropiate one, according to Zakrzewski(1987, private communication):

$$N_S = 15.78 - 18.04 \cdot \exp(-\frac{4.26}{P_1}) \quad [min^{-1}] \qquad (2.1.2.5)$$

where N_S is the frequency of the wave-generated spray splashing on the ship in cycles per minute, and P_r is the wave period. Knowing the wave period P_r and the splashing frequency N_S, the total flux of water delivered to some particular location on the ship can be calculated by the use of the following formula:

$$M = E_C \cdot LWC \cdot U \cdot \Delta t \cdot N_S \quad [kgm^{-2}s^{-1}] \qquad (2.1.2.6)$$

where E_C is the collision efficiency of water droplets with the iced object.

2.1.3 Total spray flux.

The total spray flux delivered to the ship is the sum of the wind-generated and wave-generated spray fluxes. According to Zakrzewski's study(1986) of available sea-spray data, the wave-generated spray flux is at least three times larger than the wind-generated spray flux. He also states that wind-generated spray does not affect objects located above the deck of medium sized fishing vessel (MFV-overall ship length between 35 and 50 m), therefore, only wave-generated spray needs to be considered. In the case of small fishing vessels (SFV - overall ship length less than 35 m), both spray generation processes have to be taken into account, especially as these vessels are more prone to icing.

2.2 Conditions for spray icing.

Icing at sea is dependent upon a large number of parameters. The main ones are meteorological and oceanographic parameters, such as air temperature, wind speed, sea-surface temperature, wave height and salinity. In addition, object-dependent parameters are also important. In the case of vessel icing, its size, speed, heading and activity have an effect on the amount of icing experienced.

The required conditions for sea icing are a combination of air temperature below the freezing point of sea water (about -1.8°C), and a sea-surface temperature below about +5°C. Wind speed is a factor in wave generation, and wave

height depends on it. In estimating the spray icing potential at sea, the wind speed and direction, combined with vessel speed and heading, is important. A larger wind speed relative to the ship yields more severe icing condition. The salinity of sea water is generally constant at a given location, and has a typical value of 36 parts per thousand by mass. The salinity of sea water affects the freezing temperature and the freezing process of accreted sea water.

In Canada, the greatest frequency of sea-spray icing occurs off the East Coast in winter (see Table 2.2.1) because of the proximity of open water in north-westerly flow conditions. Figure 2.2.1, from Stallabrass(1980) shows the locations of reported ship icing off the East Coast. The frequency of icing reports decreases away from the coast, reflecting the modification of arctic air, as it moves offshore. The warm water of the Gulf Stream provides a fairly clear south-eastern boundary for sea-spray icing.

Sea-spray icing conditions are typically encountered in the rear of winter cyclones, producing a strong north-westerly flow, from continental Canada to the adjacent marine area. Figure 2.2.2 from Stallabrass(1980), presents an example of a typical weather system producing spray icing conditions. It can be seen that icing conditions are generally found in the south-western quadrant of the Low, while some sheltering from icing in pack-ice is also reported. In this synoptic situation, icing conditions might

have occured elsewhere; however, no supporting reports exist.

Table 2.2.1 Percentage frequency of icing reports by accretion type (from Brown and Roeber, 1985).

Region	Total No. Obs.	Spray	Fog	Spray & Fog	*ZR/ZL	Spray & *ZR/ZL
Gulf of St. Lawrence	100	81.0	6.0	1.0	11.0	1.0
Scotian Shelf	536	94.2	0.8	0.8	2.1	2.2
Grand Banks	100	97.0	1.0	2.0	0.0	0.0
N.E. Newfoundland Shelf	233	95.9	0.0	0.0	2.8	1.4
Labrador Sea/ Davis Strait	72	86.9	1.3	10.2	0.4	0.9
Hudson Bay/ Ungava Bay	37	97.3	0.0	0.0	0.0	2.7
Eastern Arctic	69	56.4	33.3	0.0	7.3	2.9
Western Arctic	40	60.0	22.5	7.5	10.0	0.0

* *ZR/ZL* is freezing rain or freezing drizzle.

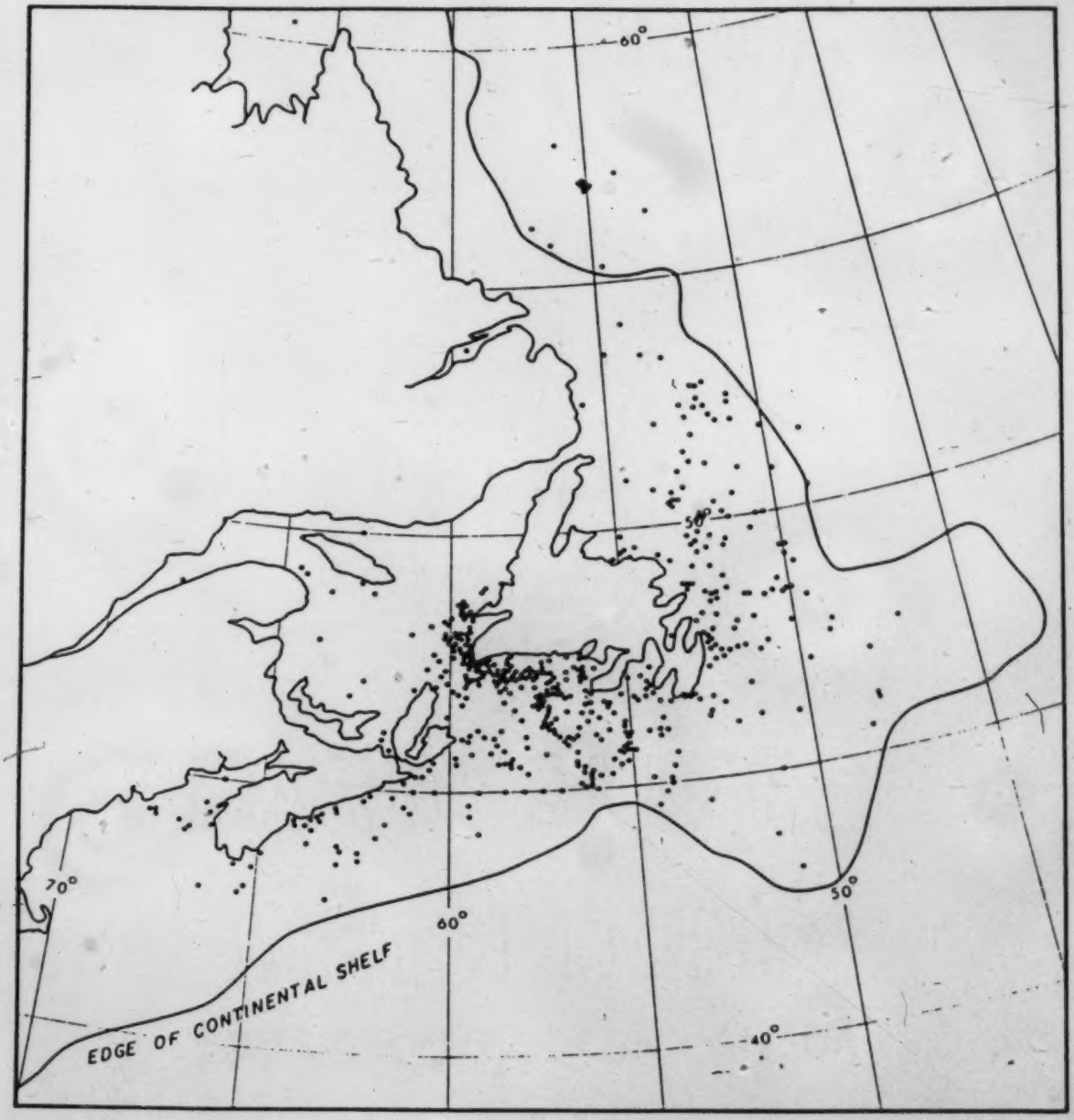

Figure 2.2.1 Location of reported ship icing off Eastern Canada between 1971 and 1979 (from Stallabrass, 1980).

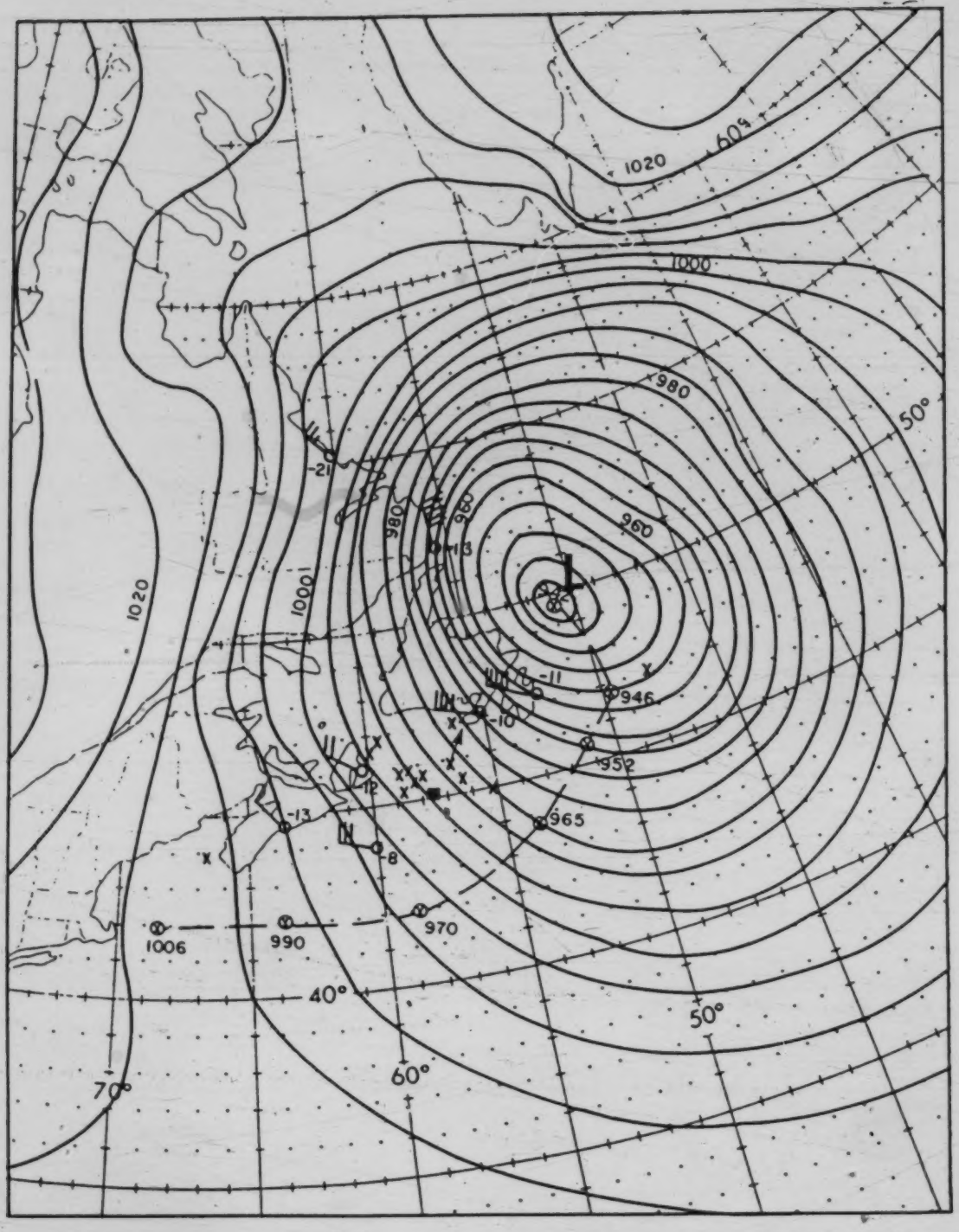

X – VESSELS EXPERIENCING ICING

■ – VESSEL IN PACK ICE – NOT EXPERIENCING ICING

Figure 2.2.2 Surface weather chart for 0600 GMT, 12 March, 1974 (from Stallabrass, 1980).

3. THE PHYSICS OF ICE ACCRETION.

In order to put the tunnel developement and icing experiments into a theoretical framework, an overview of ice accretion physics will be given here. The basic parameters which control ice accretion depend on the environmental conditions and the nature of the object exposed to these conditions. Two main problems have to be investigated. First, in order to determine the mass of brine which strikes the object, the interaction between the object and the droplets has to be examined. Second, the thermodynamic process occurring at the accreting surfacehas to be investigated, in order to determine the freezing fraction of the brine, the rate of accretion, the density and the structure of the accreted ice. In addition, the freezing process of sea water has to be discussed, since it differs significantly from that for fresh water.

3.1 Droplet - object interaction.

In order to determine the mass of droplets striking an object, it is necessary to know the field of air velocity around that object. Since we are dealing with a situation involving wind or relative air motions, the flow pattern around the iced object will control the motions of the droplets in the air. Consequently, we have to consider the mechanism of collision, and take into account the water losses from an iced object due to bouncing, partial coalescence or from shedding of water, which has been

accumulated earlier.

According to List(1977), the areodynamics of air flow around many obstacles is generally unknown. Even in the case of a cylinder, the Langmuir & Blodgett approach(1946) of using potential flow, does not reasonably describe the boundary layer effects. Viscous flow is not appropiate at higher Reynolds numbers, and potential flow is not adequate at the object-air interface. However, according to McComber(1981), potential flow is a good assumption upstream of the boundary layer separation point for small cylinders ($Re \simeq 10^4$). Experimental evidence (McComber 1981) has shown that secondary flow beyond this point is not important because its contribution to the total droplet collection is negligible.

A number of potential flow codes have been developed to describe the flow field around an object. The choice of a particular technique depends mostly on the available computing power (Lozowski & Oleskiw,1983).

The air velocity for any point around an object can be readily obtained by solving for the complex potential function:

$$F = \phi + i\psi \qquad (3.1.1)$$

where ϕ is the velocity potential and ψ is the stream function. The velocity is tangential to the curves of constant ψ, i.e. the streamlines.

S = DISTANCE BETWEEN UPPER AND LOWER TANGENT TRAJECTORIES IN UNDISTURBED FLOW AHEAD OF CYLINDER.
D = CYLINDER DIAMETER.

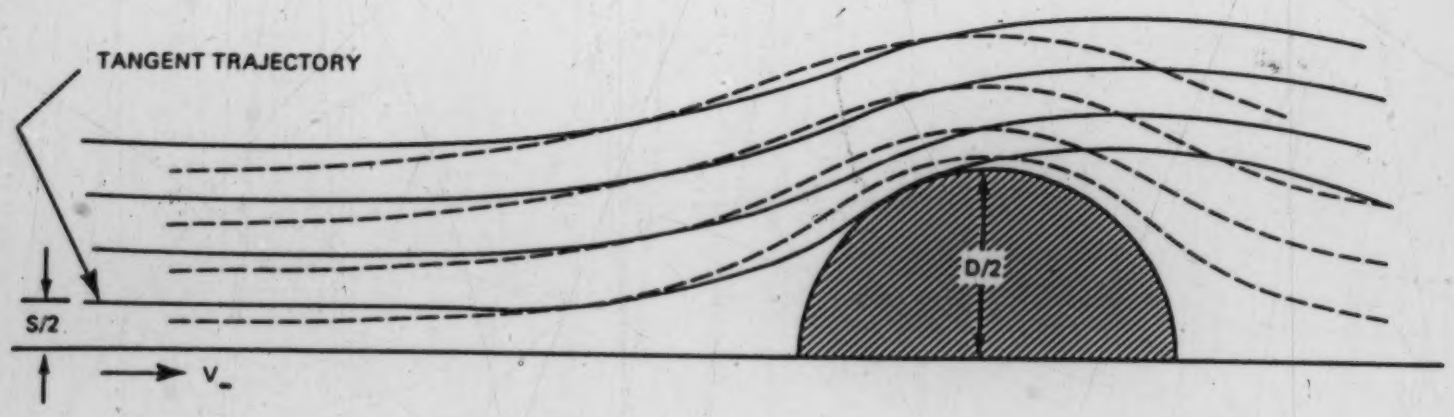

WATER DROP TRAJECTORIES
STREAMLINES

COLLECTION EFFICIENCY $E_m = \frac{S}{D}$

Figure 3.1.1 Water drop trajectories and streamlines in the vicinity of a circular cylinder (from Stallabrass, 1980).

For simple objects, such as cylinders, the dimensionless air velocity can be determined easily if the free stream velocity away from the object and the cylinder dimensions are known. Differentiating the stream function, one may determine the air velocity components at the position of the droplet's centre of mass as follows:

$$u = \frac{\partial \phi}{\partial y} \qquad v = -\frac{\partial \phi}{\partial x} \qquad (3.1.2)$$

Integrating the equation of motion for droplets in the flow field, one may determine their trajectories. Various scientists have attempted this problem in different ways. List(1977) and Lozowski & Oleskiw(1983) considered gravity, history and drag in their equations of motions, while McComber(1981), and most recently Makkonen(1985), ignored gravity and the history term, and applied the numerical solution of Langumir and Blodget(1946). The dimensionless equation of motion of a droplet in an airflow, after Langumir and Blodget is:

$$K \frac{d\bar{u}_d}{dt} = \frac{C_d Re}{24} (\bar{u}_a - \bar{u}_d) \qquad (3.1.3)$$

where K, the inertia parameter is given by:

$$K = \frac{R_d^2 \rho_w \mu_o}{9\mu D} \qquad (3.1.4)$$

and t is the dimensionless time, $\overline{u}_d$ the dimensionless droplet velocity, $\overline{u}_a$ the dimensionless air velocity, u_o the free stream velocity, Cd the droplet drag coefficient, ρ_w the water density, R_d the droplet radius and D, the cylinder diameter. The droplet Reynolds number R_e, based on the droplet's relative velocity, is given by Lozowski and Oleskiw (1983) as:

$$Re = \frac{2\rho_a R_d}{\mu}(\overline{u}_a - \overline{u}_d) \qquad (3.1.5)$$

where μ is the kinematic viscosity of air.

In order to determine the steady state drag coefficient as a function of droplet Reynolds number, the formulation of Beard and Pruppacher(1969) is frequently used:

$$\frac{CdRe}{24} = 1 - 0.189\, Re^{0.632} \qquad 21 < Re < 200 \qquad (3.1.6)$$

$$\frac{CdRe}{24} = 1 + 0.115\, Re^{0.802} \qquad 2 < Re < 21 \qquad (3.1.7)$$

$$\frac{CdRe}{24} = 1 + 0.102\, Re^{0.995} \qquad 0.2 < Re < 2 \qquad (3.1.8)$$

Since the above procedure for calculating droplet trajectories is quite complicated and time consuming, many scientists having completed these computations, introduce a fitting functions for the resulting collection efficiency curves (Langmuir & Blodgett,1946; List,1977; Makkonen,1981; Finstad et al.,1987). The collection efficiency E is defined as the ratio of the mass of droplets actually impinging on the obstacle in unit time, to the mass of droplets that would have impinged in the same time, had no deflection of droplets taken place. The solution of E, for a circular cylinder, can be presented conveniently as a function of two dimensionless parameters K (see Equation 3.1.4), and ϕ_1,

$$\phi_1 = \frac{9\rho_a D u_o}{\mu \rho_w} \qquad (3.1.9)$$

either in the form of analytical expression(Cansdale & McNaughtan,1977) or as curves(see Figure 3.1.2).

The introduction of collection efficiency into the ice accretion process is very important. This can be seen in the basic expression used to determine the icing intensity I :

$$I = E n u_o W \qquad (3.1.10)$$

where n is the freezing fraction, (i.e. the ratio of icing intensity to the mass flow of impinging water droplets), and

W is the liquid water content.

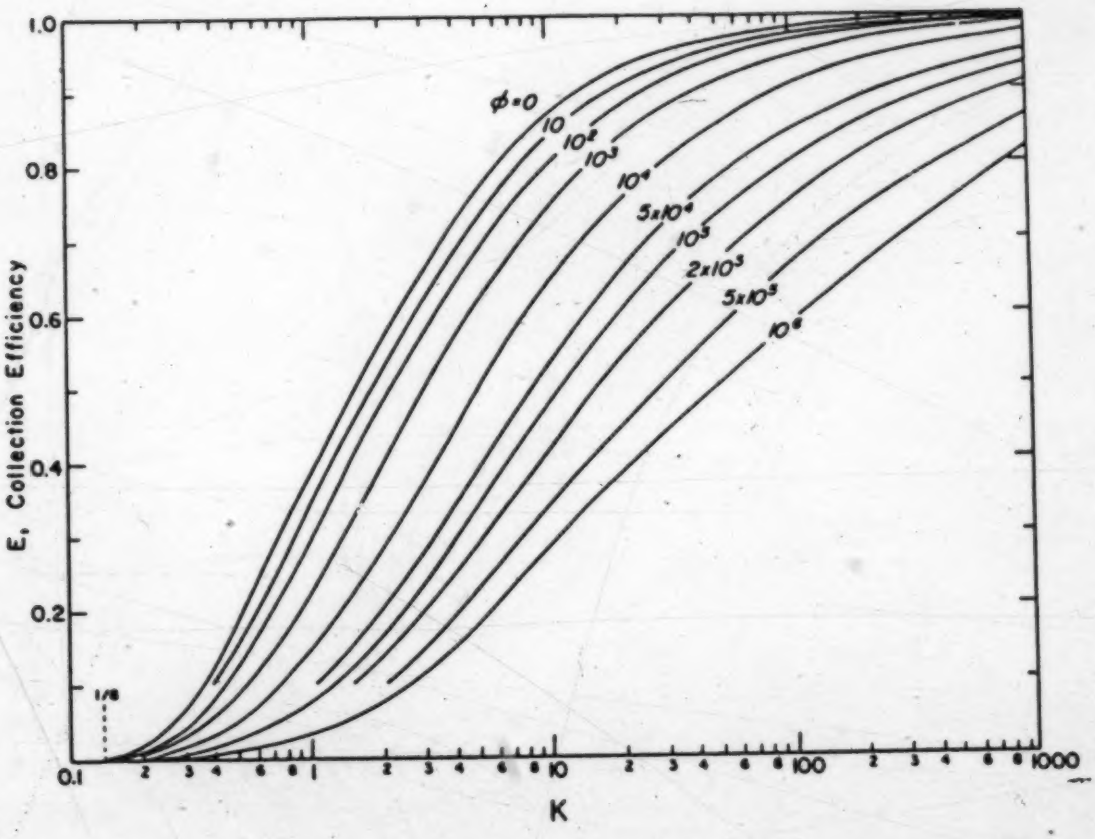

Figure 3.1.2 Collision efficiency as a function of the inertia parameter K and parameter ϕ_1, (from Minsk,1980).

Collection efficiency depends on the atmospheric parameters in such a way that E increases with increasing wind speed and droplet size, and with decreasing cylinder diameter. A serious problem in calculating E is the strong dependence on droplet diameter when the droplets are small. Therefore, the collection efficiences should be calculated separately for each size category, and a final weighted mean value of E should be used. Since this approach is computationally expensive, the median volume diameter is frequently used. Makkonen(1984), compared values of collection efficiency, calculated with typical droplet size distributions, E, with values calculated using the median droplet volume diameter, E_m, and concluded that the error involved from using E_m instead of E is neligible when E or E_m are close to 1, which is the case when the droplets are large. He also developed a relationship which can be used to correct values of E_m in the form:

$$E = 0.69\, E_m^{0.67} + 0.31\, E_m^{1.67} \qquad (3.1.11)$$

From Figure 3.1.2 one may find that, under some circumstances $E = 0$. Langmuir & Blodgett(1946) showed that this happens when $K \leq 1/8$. Therefore, the conditions for which icing theoretically does not occur (see Figure 3.1.3) may be calculated. However, as Makkonen(1984) has suggested, this

may not be fully applicable to the real world, where the air flow is turbulent and the droplets are neither of uniform diameter, nor in equilibrium with the airstream.

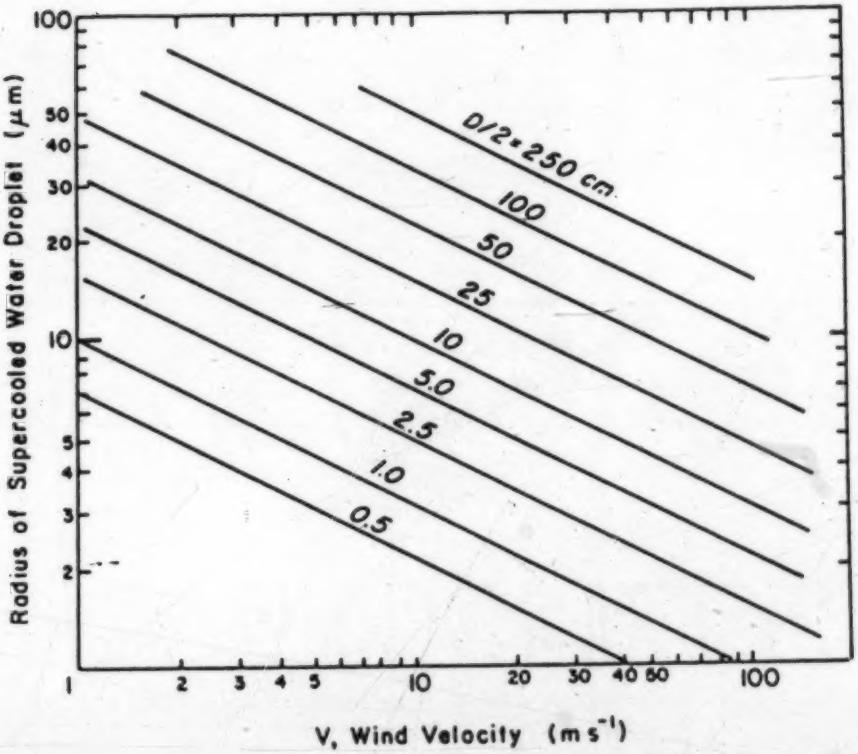

Figure 3.1.3 Critical radius D/2 of a cylinder above which icing theoretically does not occur (from Minsk, 1980).

3.2 Droplets in flight.

In atmospheric icing, the droplet temperature can be assumed to be equal to the wet bulb temperature, which, below 0°C, is close to the ambient air temperature. For sea-spray icing, this is hardly the case, since the temperature of sea water is usually much higher than the ambient air temperature, the droplets are large, and their residence in the air is brief. Therefore, it must be expected that the droplets striking a ship's surface will carry a considerable amount of sensible heat. This must be taken into account in the theoretical treatment of sea-spray icing. Under freezing sea-spray conditions, the droplet temperature will depend on the ambient air temperature, the sea surface temperature, the droplet size, and the droplet flight time before it strikes the ship's surface. Assuming a short flight time, Biot number much less than 1 and no evaporation, Stallabrass(1979) developed an analytical expression for the temperature of the droplets t_d :

$$t_d = t_a + (t_w - t_a)\exp(-k\frac{x}{U}) \qquad (3.2.1)$$

where: t_a is the air temperature; t_w is the sea surface temperature; x is the distance a droplet is carried in the air before it strikes an iced object; U is wind velocity; k is the cooling constant. The cooling constant (or

"relaxation constant") depends on droplet diameter:

$$k = \frac{6k_a Nu}{\rho_w c_w d^2} \qquad (3.2.2)$$

where: k_a is the thermal conductivity of air; Nu is the droplet Nusselt number; ρ_w is the density of water, c_w is the specific heat of impinging water and d is the droplet diameter.

The larger droplets have a lower surface-to-mass ratio and will also stay airborne for a shorter time than the smaller ones; therefore, the first will experience considerably less cooling than the second. However, any assumptions about droplet size distribution or 'effective drop diameter' and the flight time are uncertain, and the derivation of the term $-kx/v$ should be based on the observed rates of icing (Canadian Climate Centre Report, 1984).

3.3 The heat balance of an accreting surface.

The growth of ice on an accreting surface is controlled thermodynamically by the ability of the air to remove the latent heat of fusion, which is released on the surface of an object, as the accreted water freezes. Therefore, once the mass of water arriving at the accreting surface has been determined, it is necessary to investigate the heat balance of the surface, in order to evaluate what fraction of the

accreting water will freeze. The most common approach to solve the heat balance equation assumes that the ice formation is a continuous steady-state process, and that the accreting surface is in thermal equilibrium. It is also assumed that thermodynamical changes occur instantaneously. Therefore, heat transfer is always from a surface at the equilibrium temperature t_s.

After Makkonen(1984), the heat flux balance equation for the water film on an accreting surface can be written as:

$$q_f + q_v + q_c + q_k + q_a + q_n + q_l + q_s + q_i = 0 \qquad (3.3.1)$$

where:

q_f = latent heat relased in freezing;

q_v = aerodynamic heating of air;

q_c = loss of sensible heat to the air;

q_k = kinetic energy of the impinging water;

q_a = heat relased from ice cooling to the surface temperature t_s, from its freezing temperature t_f;

q_n = energy gained at the surface from short wave radiation;

q_l = heat loss or gain in warming or cooling the impinging supercooled water to the freezing temperature t_f;

q_s = net energy loss from long wave radiation;

q_i = heat loss into the ice and subsurface due to conduction.

The solution of the above equation can be readily obtained for the case of a cylinder. However, in cases of more complicated cross-sections, the physics required is very complex.

In the following discussion it is assumed that heat transfered to the surface of the iced object has a positive value. The rate of transfer of sensible heat from a cylinder is given by:

$$q_c = h\,(t_a - t_s) \qquad (3.3.2)$$

where h is the heat transfer coefficient, t_s is the equilibrium surface temperature, and t_a is the temperature of the air in the free stream. The heat transfer coefficient(after Lozowski et al., 1979) can be expressed in terms of the Nusselt number as:

$$h = k_a \cdot \frac{Nu_c}{D} \qquad (3.3.3)$$

where: k_a is the thermal conductivity of air and D is the cylinder diameter. The Nusselt number Nu_c has been found experimentally to be a function of the angle around the cylinder θ, cylinder roughness, the Prandtl number of the air (which is essentially constant and equal to 0.711), the turbulence level of the free air stream, and the cylinder

Reynolds number, Re_c, defined as:

$$Re_c = \frac{u_o D \rho_a}{\mu} \qquad (3.3.4)$$

where μ is the kinematic viscosity of air. A physical model including most of these factors has been developed by Makkonen(1984), but it is very complicated and most theoretical ice accretion studies rely on empirical approximations, based on experimental results. For the Reynolds number range from 7×10^4 to 9×10^5, Makkonen's(1984) expression for the Nusselt number, in the following form, applied to the front half of a cylinder, seems to be quite suitable:

$$Nu_c = 0.032\, Re_c^{0.85} \qquad (3.3.5)$$

For lower values of the Reynolds number (2×10^3 to 6×10^4), after List(1977), the following formula can be used:

$$Nu_c = 0.24\, Re_c^{0.6} \qquad (3.3.6)$$

The cylinder roughness during icing and the turbulence in the free stream are usually unknown. This causes uncertainity in the determination of the heat transfer coefficient. This can give rise to large errors in the

estimated heat loss. Szilder (1985), calculated that at high Reynolds numbers ($\simeq 10^6$), the error may reach 100%.

The loss of latent heat from the icing surface, q_c, will occur through evaporation of liquid water and sublimation of ice. Lozowski et al.(1979), give this term as follows:

$$q_e = h \left(\frac{Pr}{Sc}\right)^{0.63} \frac{0.622}{p\, c} L_{s,v}(e_a - e_s) \qquad (3.3.7)$$

where h is the heat transfer coefficient, Pr is the Prandtl number for air (0.711), Sc is the Schmidt number for air (0.595), $L_{s,v}$ is the latent heat of sublimation or evaporation, p is the air pressure, c_p is the specific heat of dry air at constant pressure, e_s is the saturation vapour pressure over the accretion surface at temperature t_s, and e_a is the vapour pressure in the environment.

The choice of whether to use L_s or L_v may be difficult, since both processes may take place simultaneously. However, if one urgues that a thin water film exists on the accreting surface at all times (Lozowski et al.,1979), one need only consider evaporative losses.

The air, which is decelerated in passing around the cylinder, is compressed on the upstream face of the cylinder, and this causes adiabatic heating. This, along with friction and viscous heating within the boundary layer,

may be expressed as (Schlichting, 1968):

$$q_v = hr_c \cdot \frac{U_0^2}{2c_p} \qquad (3.3.8)$$

where h is the heat transfer coefficient, r_c is the cylinder recovery factor (r_c=0.9 at the stagnation line of a cylinder), c_p is the specific heat capacity of dry air at constant pressure, and U_0 the free stream velocity.

The kinetic energy of the impinging droplet mass flux, Lozowski et al. (1979), may be expressed:

$$q_k = (EU_0w)\frac{U_0^2}{2} \qquad (3.3.9)$$

This term is very small compared to the other components of the heat balance and can be safely neglected.

The removal of heat from the impinging droplets involves three different physical processes. First, "initial freezing", takes place when a newly arrived droplet is nucleated and its temperature rises rapidly towards the freezing temperature without any significant external heat transfer. Next, the "subsequent freezing" stage, proceeds at the freezing temperature at a rate determined by the transfer of latent heat away from the droplet. Finally,

provided that the heat transfer rate is sufficiently high, a completely frozen droplet enters the "cooling phase", when its temperature drops below the freezing temperature. The heat flux in the "initial freezing" phase can be written as:

$$q_1 = (Eu_o w) c_w (t_a - t_m) \qquad (3.3.10)$$

where c_w is the average specific heat of water between t_a and t_m, t_m is the droplet freezing temperature, t_a is the droplet initial temperature. The latent heat of freezing during "subsequent freezing" can be expressed as follows:

$$q_f = I\ L_f \qquad (3.3.8)$$

where L_f is the latent heat of fusion at the freezing point and I is the icing intensity.

The heat flux in the "cooling phase" is:

$$q_a = I c_i (t_s - t_m) \qquad (3.3.12)$$

where c_i is the average specific heat of ice between temperature t_s and t_m. If the icing process is "wet", this term is zero.

The heat loss from conduction q_i, following Makkonen(1981,1984), may be neglected because of the low heat conductivity of ice, as long as the whole perimeter of the cylinder is covered by the accretion.

The heat gain or loss from short-wave radiation can also be safely neglected, since icing usually takes place under overcast conditions, and the albedo of accreted ice is high, particularly if the accreted ice is opaque.

The net longwave radiation from the accreting object is a function of air temperature, surface temperature, surface emissivity, precipitable water vapour in the atmosphere and cloud cover. A simplified expression for the net longwave radiation may be written, after Makkonen(1981), as follows:

$$q_s = \sigma a(t_a - t_s) \qquad (3.3.13)$$

where σ is the Stephan-Boltzman constant, a is equal $8.1\times10^{7}K^{3}$, t_s is the surface temperature, and t_a is the air temperature.

3.4 Solution of the heat balance equation.

The heat balance equation may be solved using several approaches. One of them, which seems to be best suited for sea-spray icing, is that of Makkonen(1984), who presented an analytical expression for n, which allows the icing rate to be determined from Equation 3.1.10. The upper limit for n is 1.0, which describes dry growth of the ice accretion. In the case of sea-spray icing which is mainly wet, n is always less than 1.0, and Equation 3.1.10 has to be solved for the surface temperature t_s, which is the equilibrium freezing temperature of water of the appropiate salinity. As ice

forms at the surface, salt is rejected from the ice crystal lattice, and the water film on the surface of the ice has a larger salt content than the arriving sea spray droplets. Since the freezing temperature of the brine, t_f, depends on the salinity S of that brine, the surface temperature, t_s, will be lower than the freezing temperature of sea water, t_f. Tabata et al.(1968), related the accretion surface temperature, t_s, to the freezing temperature of sea water, t_f, as follows:

$$t_s = (1 - n)t_f \qquad (3.4.1)$$

where the freezing temperature of sea water, t_f, is related to the salinity of sea water S as follows:

$$t_f = - 0.002 - 0.0524\, S - 6.0 \times 10^{-5}\, S^2 \qquad (3.4.2)$$

where S is in parts per thousand. Makkonen(1986), has developed a more accurate technique to find the equilibrium temperature of the accreting surface based on his theory of salt entrapment in spray ice. Nevertheless, Tabata's(1968) relationship was used for our experimental verifications because of its simplicity.

Since n is involved in the equation for the surface temperature ,t_s, and the rate of accretion I, the solution of the heat balance equation requires the application of iterative numerical methods.

Another problem arising due to spray salinity is establishing the value of the latent heat of freezing of the brine, L_s, which differs significantly from that for fresh water L_f. To date, there is little data on the latent heat of freezing of saline solutions. Schwerdtfeger(1963), has derived the following result:

$$L_s = 79.68 + 1.01\ t_f - 0.983\ S \qquad (3.4.3)$$

where t_f is the freezing temperature and S is the salinity of freezing brine. This formula is valid for salt concentrations from 20 to 40 parts per thousand. Makkonen(1986), has developed a different formula for the latent heat of freezing of salty water, which he claims, gives more realistic results than that of Schwerdtfeger(1963).

The specific heat of a saline solution and of a brine-ice mixture also differs from that for fresh water, but the incorporation of these values into the solution for the heat balance equation is not as crucial as that for the latent heat of freezing, due to the neligible magnitude of the resulting errors compared with the errors arising due to neglecting the difference between the latent heat of freezing of salty and fresh water.

4. DESIGN, CONSTRUCTION AND CALIBRATION OF THE ICING WIND TUNNEL.

For the purpose of studying the basic dynamic and thermodynamic processes which occur during the accretion of marine ice, a small, single loop, unrefrigerated wind tunnel was designed and built. The main design objectives for this outdoor marine icing tunnel were that it could be constructed at the University of Alberta, at a moderate cost, and in a relatively short time, so that the tunnel would be ready in time to conduct a number of icing experiments during the last part of the winter of 1984-1985. In order to meet these objectives, certain compromises had to be made. The available manpower suggested a simple design. The cost and time factors implied that the tunnel could not be too large. The capability of the available fan along with the requirement for a maximum wind speed of 25 m/s, dictated a maximum tunnel cross-section of 0.024 m. All of these compromises meant that large scale ice accretion and lengthy experiments were not feasible. Consequently, only a very limited spectrum of marine icing conditions could be reproduced in the icing tunnel.

4.1 Tunnel design.

The tunnel parameters are listed in Table 4.1.1, and a drawing of the tunnel is shown in Figure 4.1.1. Two views of the tunnel are shown in Figures 4.1.2a and 4.1.2b. The tunnel consists of two, short, detachable sections mounted

on wheels, so that they can be stored indoors and readily moved outdoors for experiments. This portability also facilitates de-icing of the tunnel from time to time, if too much ice accumulates on the walls.

Table 4.1.1 Tunnel parameters.

Total length	4.20 m
Length of test section	0.50 m
Height of test section	0.24 m
Width of test section	0.24 m
Test section area	0.06 m^2
Minimum air temperature	ambient
Airspeed	2 to 25 m/s
Liquid water content	1 to 10 g/m^3
Droplet size distribution *MVD*	150 ±50 μm
Fan	centrifugal 15"SISW
Drive	1.5 HP DC motor

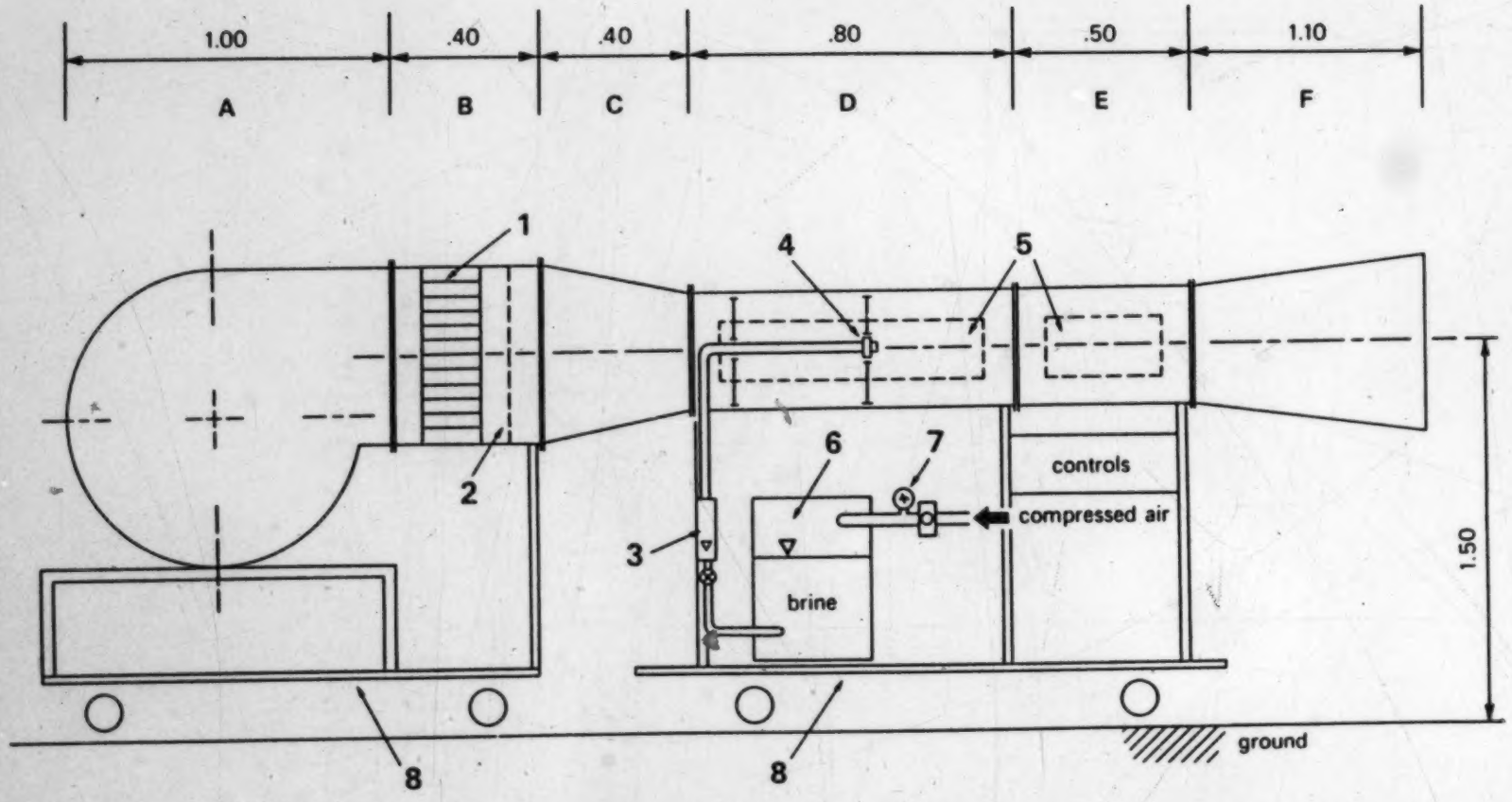

Figure 4.1.1. Schematic of the outdoor marine icing wind tunnel. Dimensions are in meters. Tunnel parts: A. centrifugal fan (1.5 HP), B. flow straighteners, C. contraction, D. spraying section, E. test section, F. outlet cone, 1. honey comb, 2. electric heater (3 kW), 3. rotameter, 4. spraying nozzle, 5. maintenance windows, 6. brine tank, 7. manometer and air pressure regulator, 8. mobile supports.

THE QUALITY OF THIS MICROFICHE IS HEAVILY DEPENDENT UPON THE QUALITY OF THE THESIS SUBMITTED FOR MICROFILMING.

UNFORTUNATELY THE COLOURED ILLUSTRATIONS OF THIS THESIS CAN ONLY YIELD DIFFERENT TONES OF GREY.

LA QUALITE DE CETTE MICROFICHE DEPEND GRANDEMENT DE LA QUALITE DE LA THESE SOUMISE AU MICROFILMAGE.

MALHEUREUSEMENT, LES DIFFERENTES ILLUSTRATIONS EN COULEURS DE CETTE THESE NE PEUVENT DONNER QUE DES TEINTES DE GRIS.

Figure 4.1.2a Overview of the tunnel with the author.

Figure 4.1.2b Tunnel test section and part of the control panel. A rotatable cylinder is skew mounted in the test section.

The tunnel was fabricated of sheet metal protected with a cold galvanizer and a coat of paint. All sections of the tunnel are square, and are joined with bolted flanges. The test-section is constructed of transparent plexiglas. In order to avoid the damaging effect of the ice accretion on the fan blades, the fan was placed on the inlet side of the tunnel. This was a compromise, since having the fan on the inlet side, caused a lot of uncontrolled turbulence, but on the other hand, even a small accretion on the fan blades could have been damaging to the fan, and may have changed the characteristics of the air flow. The fan used is a "Chicago" centrifugal fan of size 15"SISW, manufactured in the USA. It is driven by a variable speed DC motor providing controllable wind speeds of 2 to 25 m/s in the test-section. In order to diminish fan-induced turbulence in the tunnel, a flow-straightener in the form of a honey comb is used. In order to compensate for small diurnal temperature variations, a 3 kW electric heater is situated just behind the honey comb. The heater has an adjustable output. The length of the contraction (see Figure 4.1) was designed in such a way, that separation of the air flow in the spraying section was avoided.

Generally the spraying nozzles are located in the low velocity region upstream of the tunnel test-section. However, taking into account the high terminal velocities of the droplets which were to be produced, the spraying nozzle was placed downwind from the contraction in the "spraying

section" which has the same cross-section as the test-section. The spraying section has a maintenance door made of transparent plexiglas which allows easy access to and servicing of the spraying system, as well as permitting the observation of spraying nozzle performance.

The test-section, made of transparent plexiglas, has two maintenance doors which allow access to the iced object. The outlet cone was designed in such a way that the dynamic pressure loss in the tunnel was reduced by a factor of four compared to a straight outlet. This was achieved by keeping the cone expansion angle at 7°, thus avoiding stream separation at the walls.

4.2 Spraying system.

As mentioned before, in order to diminish the effect of gravity on the droplet trajectories, the spraying nozzle is located in the high speed part of the tunnel. The whole spraying system consists of a single spraying nozzle, flowmeter, insulated glass-lined brine tank, flexible brine hosing and compressed air hosing. The spraying nozzle is attached to a moveable support, so that the distance between the iced object and the nozzle can be freely adjusted. The brine is forced to flow through the nozzle by compressed air supplied to the brine tank. Unfortunately, after a long and unsuccessful search for the proper nozzle (of required flow rate, and giving the required droplet size distribution), an ordinary household sprayer nozzle was used, which

unfortunately during further testing was found not to produce a consistent droplet size distribution.

4.3 Temperature measurement.

Temperature measurements were taken at four points. Three fast response thermistors and one ordinary alcohol thermometer were used.The thermistors were used to measure the air temperature in the test section and in the spraying section just before the nozzle, and the brine temperature inside the nozzle. The alcohol thermometer was used to take the average ambient temperature. The termistors were calibrated in the laboratory in the Department of Mechanical Enginering and had an accuracy of ±0.1°C. The glass thermometer had an accuracy of ±0.5°C.

4.4 Air speed measurement.

The initial windspeed calibration was carried out in an empty tunnel. The rotational speed of the fan was correlated with the dynamic pressure, measured by use of a Pitot tube in the test-section. In this way, an ordinary *RPM* meter was calibrated in units of windspeed in the test-section. Wind velocity profiles in the test-section were obtained by the use of a Pitot tube. It was found that the flow in the test-section was generally uniform, and that deviations from the mean wind velocity across the test section were less than 5%, except near the walls. Inserting a model into the test-section created a blocking effect for which a

correction should have been made. During the experiments, the blockage effect increased with time, but the irregularity of the accreted ice shape caused difficulty in correcting the velocity. Consequently, the blocking effect of the accretion was neglected.

4.5 Liquid-water content measurement.

A direct method of liquid-water content measurement specific for a "small tunnel" has not yet been developed. Attempts were made to use several standard techniques but, mainly due to a lack of consistency and reliability of the results, an alternate method had to be used.

First, the "small rotating cylinder" method was applied. A small cylinder, 2 mm in diameter, was inserted into the test section and slowly rotated for 60 seconds. The accretion collected in this way was then weighed, and from that, the *LWC* was calculated. This method did not work, because the droplet sizes were too large comparing to the "small cylinder" diameter. Next, the "cooled cylinder" method was tried. A hollowd aluminum cylinder, .0254 m in diameter, filled with solid carbon dioxide, was inserted into the test section of the tunnel, and slowly rotated. Again, the accretion collected was weighed, and from that, the *LWC* was calculated. This method did not work either, since the large temperature difference between the wet surface of the accreted ice and the cylinder caused chipping and falling out of chunks of accretion. Measurement of the

liquid-water content and droplet size distribution using a *PMS 2-D* Grey-Scale Probe were also made, but even though the flow through the nozzle was steady and a uniform spread of spray was observed, the results were not consistent, and this method too had to be abandoned.

An alternate method, based on a knowledge of the flow rate through the nozzle (determined from the rotameter installed on the brine supply line),the angle of spray, and the assumption of uniform spread of spray was used. Following observations of the spraying system performance, it was assumed that 20% of the sprayed water was lost to the walls, and that the rest was spread uniformly accross the test-section. This was the final one employed to determine the liquid-water content in the experiments.

4.6 Droplet size distribution measurement.

The simplest method of measurement of droplet size distribution is with oil slides. Since no better method was available at the time of the experiments, this particular one was chosen. The procedure of using "oil slides" is as follows: a glass slide covered covered with ordinary motor oil is exposed to the droplet-laden airstream for a short time (approximately 5 seconds). Next, the collected droplets are photographed through a microscope. A special grid is placed on the photograph, the droplets are divided into size classes and counted. The result yields the median volume diameter, *MVD*. About 20 photographs were taken, and it was

found that the mean *MVD* for all experimental conditions was 150 micrometers with a standard deviation of 50 micrometers.

5. PROCEDURES AND EXPERIMENTS.

Icing simulation in the wind tunnel is accomplished by introducing water droplets of predetermined size and number into a cooled airstream of known speed and temperature, to produce icing conditions on an object of chosen shape. Ideally, in order to compare experimental results with analytical solutions, a state of equilibrium should exist in the test-section of the tunnel, such that:

- the droplet temperature should be equal to the ambient temperature;
- the air surrounding the droplets should be saturated;
- the spatial distribution of droplets should be uniform;
- the velocity of droplets relative to the air should be zero;
- the air stream should be non-turbulent.

All these conditions are not true at sea, and also, ideal simulation in a wind tunnel is difficult to achieve. However, the departure from ideal conditions must be understood in order to interpret the experimental results, and appreciate their limitations.

The intent was to study a number of aspects of marine icing using the experimental tunnel. Varying the airspeed, temperature and liquid water content, the following effects were observed:

- the effect of salinity on the accretion rate;
- the effect of varying air speed;
- the effect of varying air temperature;

- the effect of varying liquid water content;
- the effect of change of orientation of the accreting object;
- the physical properties of the accreted saline ice.

Also, by running parallel tests with fresh and salt water spray, an attempt was made to estabilish "scaling coefficients" due to salinity.

5.1 Procedures

The experimental procedures included fresh water or sea water preparation, tunnel assembly, preparation of the measuring equipment and documentation, pre-experimental tunnel calibration and tunnel initialization, the experiments, tunnel clean-up and disassembly.

The sea-water was prepared from distilled water and dehydrated sea salt, "Marina mix" (for the composition see Apendix A1), supplied by the Department of Biology of the University of Alberta. This was done well ahead of time, as about two days were needed to fully dissolve all sea salts at room temperature. The sea water or fresh water were then stored overnight in a cold room, so that the water temperature during the experiments was near freezing.

The pre-experimental tunnel calibration and tunnel initialization included setting of the water flow rate through the spraying nozzle, setting the flow rate of air in the test-section, checking the ambient temperature reading and adjusting the heater output.

Experiments, documented in the later part of this chapter, were carried out as follows:

1. The flow rate through the nozzle of fresh water or brine of known temperature was adjusted;
2. The air flow rate through the test-section of the tunnel was adjusted;
3. The ambient air temperature was measured;
4. The model, a hollow aluminum cylinder .0254m in diameter, cooled to the ambient temperature, was inserted into the test section for ten minutes.
5. The temperature was taken and recorded every minute, at all measuring points.
6. At the end the ten minute experiment, the model with its accretion was quickly taken out of the test section, photographed, and measured.
7. A ten centimeter long part of the accretion was cut out from the middle and weighed.
8. The tunnel was cleaned up, and either initialized again for another experiment, or disassembled.

5.2 Experiments.

A major drawback of an open tunnel is the lack of air temperature control and, therefore, a dependence on environmental conditions. Delays in the completion of the tunnel, coupled with a few breakdowns and an early spring, did not allow a great number of experiments to be performed during the winter of 1984-85. The experimental conditions

and results are summarized in Table 5.2.1. There were about twice as many experiments carried out as those listed, but the remainder were discarded for various reasons.

Table 5.2.1 List of experiments and experimental conditions.

Position of the tested model	Wind speed V = 15 m s^{-1} LWC = 5 g m^{-3} MVD = 150 μm			
	Pure Water		Salty Water	
	1	2	3	4
Horizontal	T_1 = -11.3°C	T_1 = -5.7°C	T_1 = -11.1°C	T_1 = -4.6°C
	T_2 = -11.4°C	T_2 = -7.8°C	T_2 = -12.6°C	T_2 = -6.5°C
	T_3 = 0.9°C	T_3 = 3.2°C	T_3 = 3.2°C	T_3 = 11.0°C
	m = 75.9 g	m = 58.1 g	m = 123.6 g	m = 54.5 g
	5	6	7	8
Skew Horizontal	T_1 = -9.0°C	T_1 = -5.6°C	T_1 = -11.0°C	T_1 = -5.7°C
	T_2 = -11.4°C	T_2 = -7.7°C	T_2 = -12.0°C	T_2 = -6.2°C
	T_3 = 0.8°C	T_3 = 3.3°C	T_3 = 2.2°C	T_3 = 8.7°C
	m = 78.1 g	m = 50.7 g	m = 92.5 g	m = 44.1 g
	9		10	
Vertical	T_1 = -10.6°C		T_1 = -7.5°C	
	T_2 = -11.1°C		T_2 = -7.7°C	
	T_3 = 2.2°C		T_3 = -1.2°C	
	m = 74.1 g		m = 61.0 g	

continued...

Table 5.2.1 continued:

Position of the tested model	Wind speed V = 10 m s^{-1} LWC = 5 g m^{-3} MVD = 150 μm			
	Pure Water		Salty Water	
Horizontal	11		12	13
	T_1 = -7.8°C		T_1 = -9.9°C	T_1 = -3.1°C
	T_2 = -8.9°C		T_2 = -12.3°C	T_2 = -6.5°C
	T_3 = 2.5°C		T_3 = -0.5°C	T_3 = 7.7°C
	m = 63.2 g		m = 105.5 g	m = 45.6 g
Skew Horizontal	14	15	16	17
	T_1 = -4.3°C	T_1 = -7.4°C	T_1 = -10.0°C	T_1 = -4.8°C
	T_2 = -9.5°C	T_2 = -8.9°C	T_2 = -12.3°C	T_2 = -6.5°C
	T_3 = 1.2°C	T_3 = 1.8°C	T_3 = -0.2°C	T_3 = 7.7°C
	m = 90.0 g	m = 56.5 g	m = 91.8 g	m = 48.0 g
Vertical	18			
	T_1 = -5.6°			
	T_2 = -9.4°C			
	T_3 = -0.2°C			
	m = 52.3 g			

continued...

Table 5.2.1 continued:

Position of the tested model	Wind speed V = 10 m s^{-1} LWC = 7.5 g m^{-3} MVD = 150 μm		
	Pure Water		Salty Water
	19	20	21
Horizontal	T_1 = -7.0°C T_2 = -10.0°C T_3 = -1.0°C m = 52.6 g	T_1 = -6.7°C T_2 = -8.6°C T_3 = 3.9°C m = 53.0 g	T_1 = -10.0°C T_2 = -12.2°C T_3 = -0.8°C m = 77.5 g
	22	23	24
Skew Horizontal	T_1 = -7.5°C T_2 = -10.1°C T_3 = -0.4°C m = 51.9 g	T_1 = -6.7°C T_2 = -8.6°C T_3 = 2.7°C m = 60.1 g	T_1 = -8.9°C T_2 = -11.2°C T_3 = -1.1°C m = 94.0 g
	25		26
Vertical	T_1 = -10.2°C T_2 = -10.9°C T_3 = -1.0°C m = 61.0 g		T_1 = -7.0°C T_2 = -8.1°C T_3 = -2.3°C m = 50.1 g

T_1 - temperature in the test section (not very reliable because of icing on the temperature sensor).

T_2 - temperature of dry air.

T_3 - temperature of brine

m - mass of accretion accumulated on the middle 10 cm of tested cylinder of diameter 25.4 mm.

The experiments with fresh water spray were carried out in the University's refrigerated FROST tunnel.

The experiments themselves were ten-minute continuous accretions on a 0.0254m diameter aluminum cylinder. The cylinder was not rotated. The liquid water content in the experiments was either 5g/m³ or 7.5g/m³. These are not representative values for marine sea spray, and under marine conditions the spray is more likely to be intermittent than continuous. The spectrum had a median volume diameter of 150 micrometers calculated from oil slides. This value is perhaps somewhat small for "typical" marine conditions. Nevertheless, it was about the largest size feasible with the available nozzle, and the limitations of tunnel geometry. With a small horizontal tunnel, such as the one used for these experiments, the problem arises that very large droplets, even if produced by the nozzle, simply fall out of the airstream before they impinge on the accreting object.

Two wind speeds were used in the experiments, 10m/s and 15m/s. Three different orientations were also employed: a horizontal cylinder; a vertical cylinder; and a skew horizontal cylinder at 45° to the airstream. Due to the outdoor nature of the tunnel, several different temperatures were used during the experiments, ranging from -6.2°C to -12.6°C.

6. RESULTS AND DISCUSSION.

A number of icing experiments using fresh and salty water were carried out. From all the experiments, only twenty-six were selected as being meaningful and of reasonable accuracy. The remaining experimental results were thought to be of insufficient quality, mainly due to the malfunction of the spraying system, or in some cases, due to improper timing. There were also a few cases when the fan could not produce the required air flow rate, the mass of accretion could not be measured or the temperature readings were not reliable.

The sensitivity of the icing to air temperature, coupled with a limited ability to control the temperature, made it difficult to make precise comparisons between individual experiments. Nevertheless, some study objectives were achieved, and certain qualitative observations can be made based on the experiment results.

6.1 Effect of cylinder orientation.

There were six cases where the air temperature in the horizontal and skew horizontal orientations were within 0.5°C of each other. For these cases, the average mass ratio (horizontal/skew horizontal) was 0.92. This value is higher than the value of 0.71 which one would expect based on the cosine of the inclination angle. Therefore, there may be a tendency for a smaller fraction of the impinging water to be shed from the skew cylinders. This contrasts with the

results from experiments on rotating cylinder carried out by Lozowski and Makkonen in the summer of 1985 (Lozowski, private communication), who found that the cosine law behaviour for the accreted mass was followed quite closely. Only two cases could be compared for the vertical orientation. In these cases, the mass ratios (vertical/horizontal) were 0.95 and 0.58 for an average of 0.77. This result is clearly not statistically significant. However, it is notable that in both cases, the masses in the vertical orientation were less than those in the horizontal orientation. Consequently, it would seem that the effect of water flow down the cylinder under gravity needs further investigation.

6.2 Effect of varying the liquid water content.

There were four comparable cases at the two liquid water contents, 5g/m³ and 7.5 g/m³. The mass ratios in these cases were 0.84, 0.73, 0.58 and 0.94, giving an average of 0.77. Since this is the ratio of the mass accreted at 5 g/m³ divided by the mass accreted at 7.5 g/m³, the results appear to suggest that the accreted mass decreased with increasing liquid water content in the experiments. This may be a real physical phenomenon, or, more likely, it is a result of the way the liquid water content was calculated. The liquid water content calculations have not been verified, and could have been inaccurate.

6.3 Effect of varying wind speed.

There were four cases which were comparable at the two wind speeds. The mass ratio average for these cases was 0.94 suggesting only a slight influence of wind speed on the accretion rate. This may be due to a small difference between the two wind speeds tested.

6.4 Effect of air temperature.

By ignoring the orientation and wind speed effects (except for the vertical orientation), it is possible to use all of the results to plot a graph showing the effect of temperature on the accretion rate (see Figure 6.4.1). Using a least squares fitting technique, straight lines were drawn through the resulting points. Interestingly, the linear fit for the saline cases lies above that for the fresh water cases. This result may suggest that a large amount of unfrozen brine is caught in the more porous salty accretions. The lines cross at approximately -7°. This does not have any physical meaning as it happens at the edge of the temperatures tested, and also the lines were forced to pass through 0°C for the fresh water cases, and -1.8°C for the saline cases.

6.5 Differences in accretion appearance.

The saline ice, when first removed from the tunnel, was quite soft, fragile, and squishy, suggesting that it cointained quite a bit of unfrozen brine in a spongy matrix.

Further examination proved that the saline ice was indeed much spongier than the pure ice. The salty accretion, after being left for a while, released the unfrozen brine. The remaining pure ice was much lighter than it had been immediately after experiment. This may be the explanation of the observed mass differences. An examination of the photographs of the ice accretions allows some characteristic features for salt and fresh water accretions to be inferred. The salinity effect is quite apparent in the photographs (see Figures 6.5.1 to 6.5.4). The brine accretions are all milkier in appearance and more massive than their freshwater counterparts. They also seem to be somewhat rougher. If this roughness enhances the heat transfer, it may help to explain why the accreted mass is greater in the saline cases. The effect of gravity resulted in an asymmetrical accretion with icicles on the horizontal cylinder, and a variation of thickness with height on the vertical cylinder. In the brine cases the gravity effect is much more pronounced than in the freshwater cases.

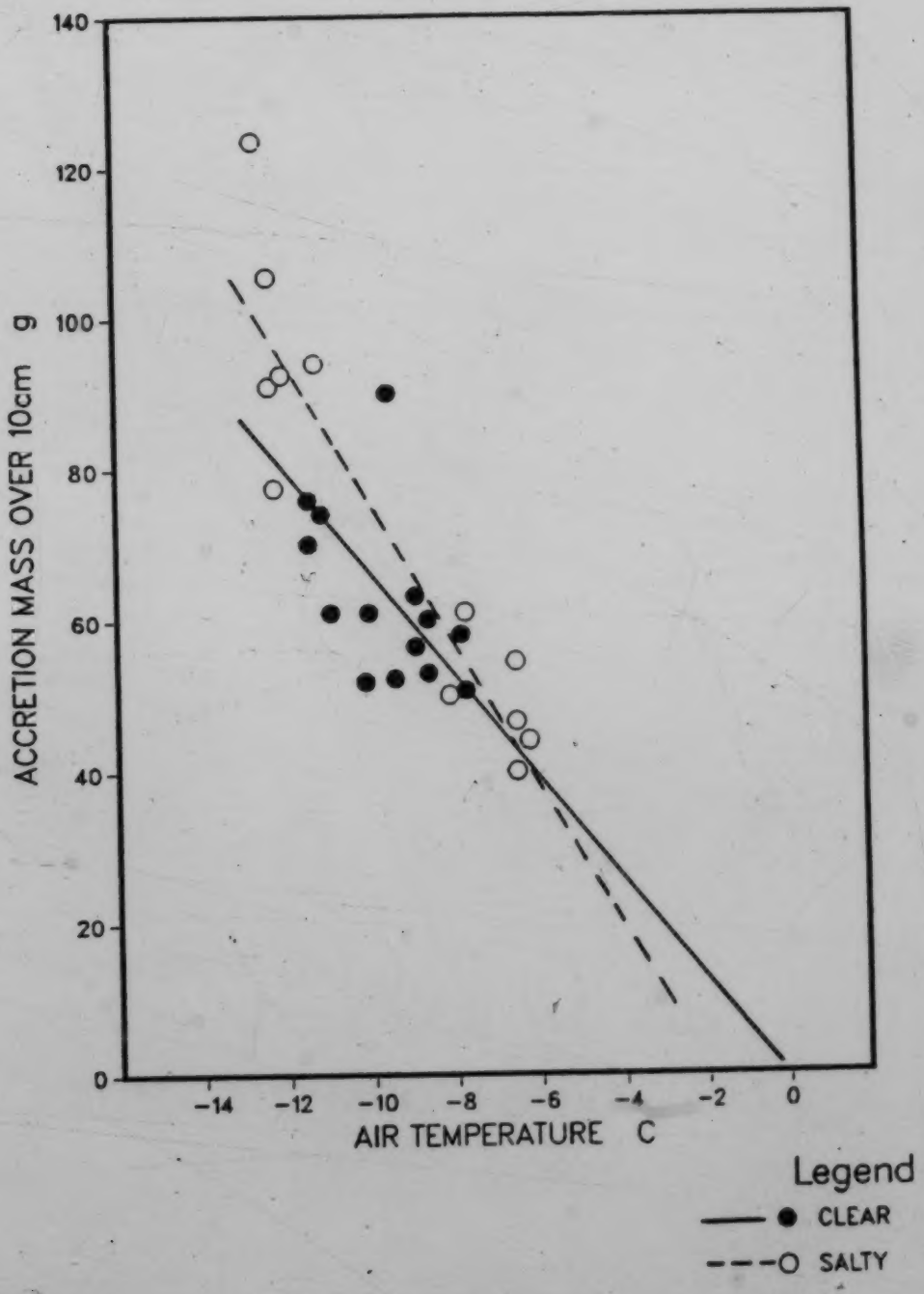

Figure 6.4.1 Accretion mass as a function of ambient air temperature for fresh and sea water cases.

Figure 6.5.1 Ten minute fresh water accretion(case #1).

Figure 6.5.2 Ten minute salt water accretion(case #3).

Figure 6.5.3 Profile of ten minute fresh water accretion(case #1).

Figure 6.5.4 Profile of ten minute salt water accretion(case #3).

6.6 Comparison between the experimental results and the numerical simulations.

A time-dependent model of ice growth on the front half of a nonrotating cylinder under spray icing conditions was used. This numerical approach generally follows that of Makkonen (1984), with the implementation of the Stallabrass' (1980) formula for droplet temperature change in flight, and Tabata's (1968) formula for the equilibrium temperature of the saline ice accreting surface. The Fortran program for the model is listed in Appendix A2.

The input parameters are: wind speed, air temperature, spray temperature, median volume drop diameter, liquid water content and cylinder diameter. The collision efficiency was determined from the empirical equation of Langmir and Blodget (1946). The energy balance of the cylinder was solved for the freezing fraction, to determine the mass of ice accreted, and then for the equilibrium surface temperature. It was assumed that the ice accreted on the front half of the cylinder was distributed uniformly around the cylinder, to give an increase in the cylinder diameter and ice load at each time step. This did not correspond with the way ice was accreting during the experiments but it was a simplification.

A comparison between the numerical simulation results and the experimental results is shown in Figure 6.6.1 for fresh water spray and in Figure 6.6.2 for brine spray. From those figures it is evident that the numerical simulation

for salty water cases underestimates the mass of the ice accretion by a larger degree than for the fresh water cases. For the fresh water spray, the model underestimates the amount of accretion only by 12.5% on average, while in the case of brine spray, the underestimate is 41.7%. This large underestimate for the brine cases can be explained in part by the large unfrozen water content found in the salt water accretions, which the model does not account for. The underestimate for fresh water cases may also be the result of liquid water entrapped in fresh water accretion. This phenomenon is known as "spongy ice."

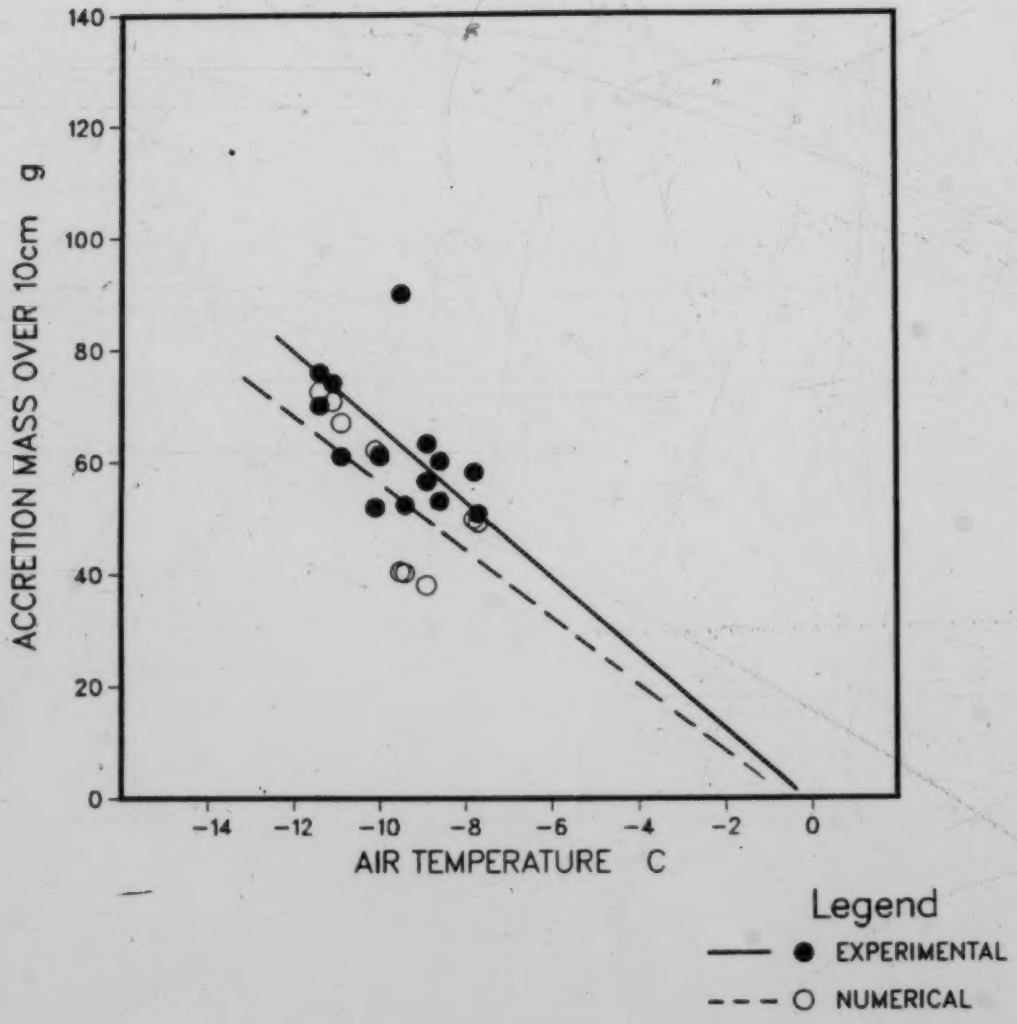

Figure 6.6.1 Accretion mass as a function of ambient air temperature for experimental and numerical simulation of fresh water icing.

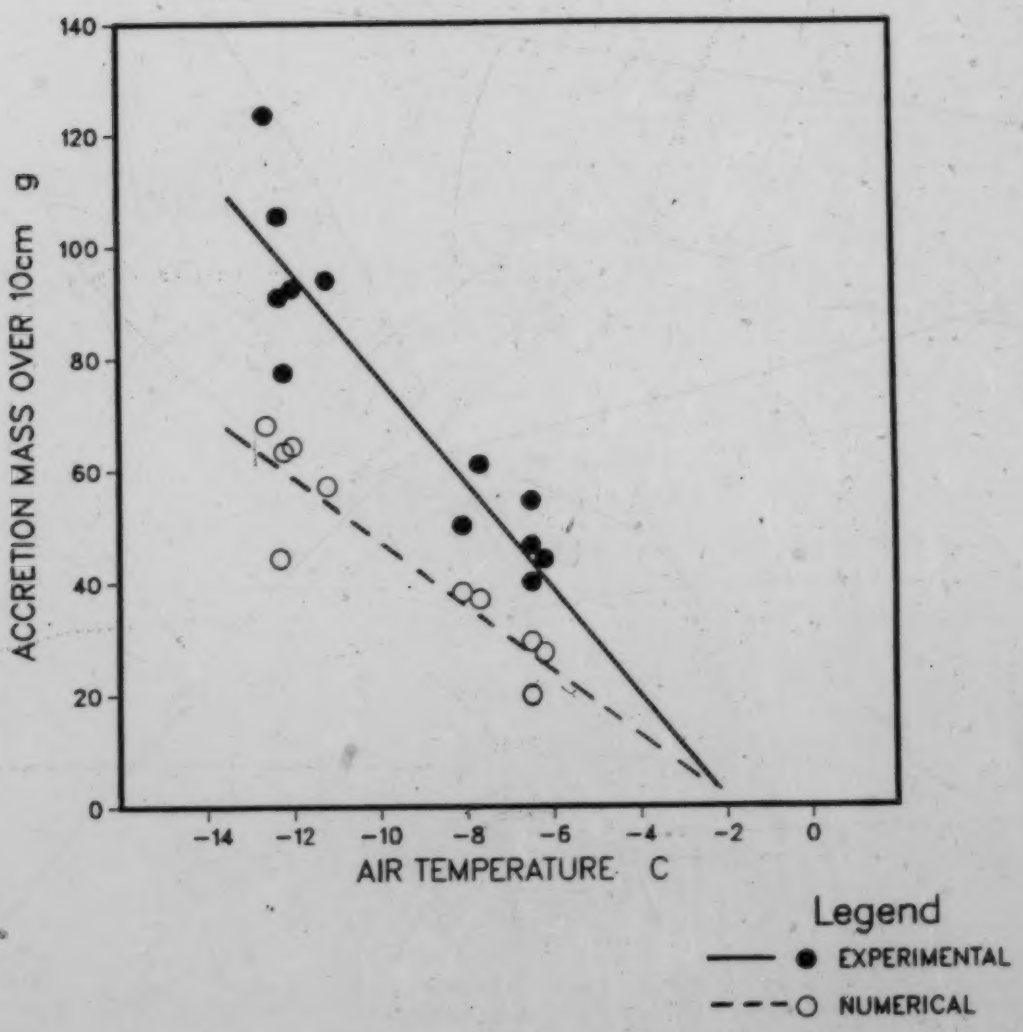

Figure 6.6.2 Accretion mass as a function of ambient air temperature for experimental and numerical simulation of salty water spray icing.

7. SUMMARY, CONCLUSIONS AND SUGGESTIONS FOR FUTURE STUDY.

In order to be able to simulate marine ice accretion and examine its properties, an outdoor icing wind tunnel has been constructed. This tunnel was the first of its kind in Canada, and one of the first in the world. Although small, and susceptible to the vagaries of the weather, it allowed a number of preliminary icing experiments to be carried out. These shed some light on the differences between salty and fresh water accretions.

Based on the limited number of experiments, it is impossible to draw firm conclusions. However, the experiments completed indicate certain trends which need to be examined more carefully. These are:

9. Variations in the cylinder orientation do not appear to significantly affect the accretion rate.
10. Small wind speed changes (from 10 m/s to 15 m/s) do not affect the accretion rate significantly; however, there is a suspicion that the spray distribution across the tunnel was affected by air speed, and hence the validity of this result is in question.
11. Under the conditions tested, the accretion mass varies almost linearly with the temperature depression below the freezing point.
12. Contrary to expectation, the accretion rates decreased with increasing liquid water content. This result may be attributed to the way the liquid water content was calculated, and this needs further examination.

13. The rates of accretion for brine are larger than for pure water. A full explanation of this difference is not available yet; however, several tentative explanations may be offered:
    a. Saline accretions tend to be rougher, possibly giving rise to an enhanced heat transfer;
    b. Saline accretions are spongier than pure accretions; that is, a large amount of unfrozen water is caught in the porous structure of saline accretions. This is supported by the following two observations:
        1) The saline accretion are softer, milkier in appearance, and more fragile than the freshwater accretions.
        2) The numerical simulations when compared with experimental results, suggest that there may be a large liquid water content in the saline accretions;
    c. Saline accretions appear to be more asymmetrical (smaller at the top and larger at the bottom) and grow bigger icicles;

Other conclusions may be drawn with regard to tunnel construction and tunnel applicability to sea spray icing experiments.

1. Even though the tunnel was designed using sound engineering knowledge, the scale of the real phenomenon cannot be reproduced in the tunnel. Since scale is a factor of major importance, the tunnel applicability to

full-scale simulation of sea-spray icing is questionable.

2. There is a need to design a spraying system which will produce spray of the required characteristics.
3. Having the tunnel outdoors causes serious inconveniences in tunnel maintenance (the operating personnel, and the tunnel instrumentation are exposed to harsh weather conditions). This could be solved by installing the tunnel indoors, but allowing it to suck in outdoor air. The tunnel would then have to be insulated.
4. The small cross-section of the tunnel does not allow for lengthy experiments due to an increasing blockage effect which needs to be examined more closely.

A number of suggestion to improve the experimental procedure can be given:

1. In order to make more sound comparisons between the numerical simulation and the wind tunnel simulation, the accreting cylinder should be rotated.
2. A more precise method for determining the liquid water content and droplet size distribution of the spray should be developed.
3. A standard nozzle, producing a spray with the required parameters should be found, to enable similar experiments to be carried out in different tunnels.
4. In order to simulate sea-spray icing more realistically, intermittent spraying should be used.

BIBLIOGRAPHY.

Brown, R.D. and P. Roeber, 1985: "The ice accretion problem in Canadian waters related to offshore energy and transportation." *Canadian Climate Centre Report* 85-13, 295p

Beard, K.V. and H.R. Pruppacher, 1969: "A determination of the terminal velocity and drag of small water drops by mins of wind tunnel." *Journal of the Atmospheric Sciences*, No. 76, 1066-1072p.

Borisenkov, E.P. and V.V. Panov, 1974: "Basic results and prospects of research on hydrometeorological conditons on shipboard." *Cold Region Research and Engineering Laboratory*, Technical Translation No. 411, 1-30p.

Cansdale,J.T. and I.I. McNaughtan, 1977: Calcuation of surface temperature and ice accretion rate in mixed water dropet/ice crysta cloud." *Royal Aircraft Establishment* Technical Report No. 77090. "Mobil Platform Stability". *Norwegian Hydrodynamic Laboratories* MOPS Report No. 15, 56p

Finstad, K.J., E.P. Lozowski and E.M. Gates, 1987: "A computational investigation of water droplet trajectories". *Journal of Atmospheric and Oceanic Technology (In press).*

Horjen, I. and S. Vefsnmo, 1984: "Mobile Platform Stability.",*MOPS* Subproject No. 02 - Icing. *Norwegian Hydrodynamic Laboratories*. Report No. NHL 284002, 56p.

Itagaki, K., 1977: "Icing on ships and stationary structures under meritime conditions." *Cold Region Research Laboratory*. U.S.A., Special Report No. 77-27.

Jessup, R.G., 1985: "Forecast techniques for ice accretion on different types of marine structures, including ships, platforms and coastal facilities." *Marine Meteorology and Related Oceanographic Activities* Report No. 15, p. 90.

Katchurin, L.G., Gashin, L.I. and I.A. Smirnov, 1974: "Icing rate of small displacement fishing boats under various hydrometeorological conditions." *Meteorologija i Hydrologija* No. 3, p. 50-60.

Langumir, I and K.B. Blodgett, 1946: "Matematical Investigations of Water Droplet Trajectories." *G.E. Report* R1244. Reprinted in Collected Works of I. Langmuir, Pergamon Press, p.335-393.

List, R., 1977: "Ice Accretion on Structures." *J. of Glaciology*, Vol. 19 No. 81, p. 451-465.

Lozowski, E.P. and M.M. Oleskiw, 1983: "Computer Modeling of Time-Dependent Rime Icing in the Atmosphere." *CRREL Report 83-2*, p. 74.

Lozowski, E.P., Stallabrass, J.R. and P.F. Hearty, 1979: "The icing of an unheated non-rotating cylinder in liquid water droplet-ice crystal clouds." *National Research Council Canada* LTR-LT-96 p. 109.

Lozowski, E.P. and E.M. Gates., 1985: "Marine icing models: how do they work and how good are they? " *Proceeding of Int'l Workshop on Offshore Wind and Icing* Halifax, Nova Scotia, October 7-11, p. 102-122.

Makkonen, L.,1981: "Estimating Intensity of Atmospheric Ice Accretion on Stationary Structures". *Journal of Climate and Applied Meteorology*, p. 929-939.

Makkonen, L. and J.R. Stallabrass, 1984: "Ice accretion on cylinders and wires." *National Research Council Canada* LTR-LT-005 p. 43.

Makkonen, L., 1984: "Modelling of ice accretion on wires." *Journal of Clim. and Appl. Met.* Vol. 23, No. 6, p. 929-939

Makkonen, L., 1985: "Heat transfer and icing of a rough cylinder." *Cold Regions Science and Technology*, 10(1985) p. 105-116 Elsevier Science Publishers B.V., Amsterdam, Netherland.

Makkonen, L., 1986: "Salt Entrapment in Spray Ice." *IAHR* Ice Symposium 1986, Iowa City, Iowa, U.S.A., p. 165-178.

McComber, P., 1981: "Numerical simulation of ice accretion using the finite element method." *Sixth Int'l Conf. on Port and Ocean Engineering under Arctic Conditions* (POAC), Quebec, July 27-31, p. 1047-1056

Minsk, L.D., 1977: "Ice accumulation on ocean structures." *CRREL* Report No. 77-17 p. 46.

Schlichting, H., 1968: "Boundary Layer Theory". Sixth Edition. *McGraw-Hill*, New York, 747p.

Shellard, H.C., 1974: "The meteorological aspects of ice accretion on ships." *World Meteorological Organization*, Report No. 10, WMO No. 397 Geneva, Switzerland, p. 34.

Stallabrass, J.R., 1971: "Meteorological and oceanographic aspects of trawler icing off the Canadian east coast." *Marine Observer*, Vol. 41 p. 107-121.

Stallabrass, J.R., 1979: "Icing of Fishing Vessels: An Analysis of Reports from Canadian East Coast Waters." *National Research Council of Canada*, Division of Mechanical Engineering, Laboratory Technical Report LTR-LT-98 p. 52.

Stallabrass, J.R., 1980: "Trawler icing: a compilation of work done at N.R.C." *N.R.C.*, Mechanical Eng. Report MD-56, No. 19372, Ottawa, Canada, p. 103.

Szilder, K., E.P. Lozowski, E.M. Gates, 1986: "A new time dependent ice accretion model for non-rotating cylinders. *Proceedings of the 8th IAHR Ice Symposium*, Iowa City, Iowa, Vol. III, p. 179-194.

Tabata, T., S. Iwata and N. Ono, 1968: "Studies of ice accumulation on ships." Part I. *National Research Council of Canada Technical Translation 1318* NRC TT-1316, p. 42.

Zakrzewski, W.P., 1986: "Icing of ships." NOAA Technical Memorandum, ERL PMEL-66, *Pacific Environmental Laboratory*, Seattle, WA, p. 74.

APPENDIX A1

COMPOSITION OF SEA SALT USED IN EXPERIMENTS.

RILA MARINE MIX (Syntetic Sea Water Compound), produced by *RILA PRODUCTS* from Teaneck, N.J. 07666, USA, was used, to prepare sea water for sea spray icing experiments. 1 lb of *RILA MARINE MIX*, when dissolved in 3 gallons of tap water, produces a solution having the following typical analysis (from *RILA PRODUCTS* TECHNICAL BULLETIN # 343):

COMPONENT	ppm (by mass)
Cl^-	19130.
Na^+	10460.
SO_4^{--}	2600.
Mg^{++}	1260.
Ca^{++}	490.
K^+	348.
Tris Amino	32.
Br^-	27.
BO_3^{---}	12.
I^-	8.97
Sr^{++}	3.50
Mn^{++}	.50
F^-	.40
Zn^{++}	.20
Fe^{+++}	.10
Co^{++}	.07
Al^{+++}	.03
MoO_4^{--}	.02

APPENDIX A2

FORTRAN PROGRAM LISTING FOR THE MODEL OF SPRAY ICE ACCRETION ON A NON-ROTATING CYLINDER.

```
      DIMENSION TS(600),R(600),RT(600),E(600),ES(600)
      REAL LWC,V,TA,TS,TF,N,E,ES,Z,EM,TW,TD,RE,NU,NUC,K,KO

C     ..... INPUT VARIABLES FROM KEYBOARD .....
C     LWC.....LIQUID WATER CONTENT g/m³
C     V..... WIND SPEED m/s
C     TA.....AMBIENT AIR TEMPERATURE °C
C     TW.....SPRAY TEMPERATURE AT THE NOZZLE °C
C     DD.....DROPLET MEAN MASS VOLUME DIAMETER micrometers
C     S.....SPRAY SALINITY parts per tousand by mass

      READ(5,LFMT)LWC,V,TA,TW,DD,S

C     TF....FREEZING TEMPERATURE DEPENDING ON SPRAY SALINITY S

      TF=-.2E-2-.0524*S-.6E-6*S*S

C     .....MODEL VARIABLE.....
C     DC.....ICED CYLINDER DIAMETER m
C     RD.....DROPLETS REYNOLDS NUMBER
C     NU.....DROPLETS NUSSELT NUMBER

      DC=.0254
      RD=DD*V/(1.5E2)
      CO=.087*RD**(.76*RD**(-.027))+1
      NU=.37*RD**.6

C     EA.....WATER VAPOUR SATURATION PRESSURE AT TA
C     ET.....WATER VAPOUR SATURATION PRESSURE AT TW

      EA=(((1.9226E-7*TA+2.4545E-5)*TA+1.4224E-3)*TA+.044436)
     *TA+.6109
      ET=(((1.9226E-7*TW+2.4545E-5)*TW+1.4224E-3)*TW+.044436)
     *TW+.6109
      XT=1.+154.73*(EA-ET)/(TA-TW)

C     TD..DROPLET TEMPERATURE AFTER IT PASSED DISTANCE BETWEEN
C     ..... NOZZLE AND ICED CYLINDER .....

      TD=TA+(TW-TA)*EXP(-.375E5*NU*XT/(DD*DD*V))
```

```
      MODEL  INITIALIZATION  AND  ACCRETION  MASS  INTEGRATION;
      TIME STEP = 10 s
      TS(I)..ACCRETING SURFACE EQUILIBRIUM TEMPERATURE AT EACH
      TIME STEP
      N.....................................FREEZING FRACTION
      ES(I).. WATER VAPOUR SATURATION PRESSURE OVER ACCRETING
      SURFACE AT EACH TIME STEP
      R(I)..............  ACCRETION MASS DURING EACH TIME STEP
      RT(I)..... INTEGRATED ACCRETION MASS OVER "I" TIME STEPS
      RE    - ICED CYLINDER REYNOLDS NUMBER (NOTE DC CHANGE AS
      ICE ACCREATES)
      K.....................................INERTIA PARAMETER
      E(I).....OVERALL COLLECTION EFFICIENCY AT EACH TIME STEP
      EVL.............MASS OF BRINE COLLECTED AT EACH TIME STEP

      DO 50 I=10,600,10
      R(I)=.0
      RT(I)=.0
      TS(I)=TF
      E(I)=.0
50     CONTINUE
      DO 100 I=10,600,10
      IF(N.GE..0001)TS(I)=(1.+N)*TF
      ES(I)=(((1.9226E-7*TS(I)+2.4545E-5)*TS(I)+1.4224E-3)*TS(I)
      +.044436)*TS(I)+.61094
      RE=DC*V/(1.5E-4)
      NUC=.032*RE**.85
      H=.025*NUC/DC
      K=V*DD**2/(9.E4*DC)
      KO=K/CO
      IF(KO.LE.1.25E-2)EM=.001
      IF(KO.LE..8)EM=.5*(ALOG10(8*KO))**1.6
      IF(KO.GT..8)EM=KO**1.1/(KO**1.1+1.426)
      E(I)=.69*EM**.67+.31*EM**1.67
      EVL=E(I)*V*LWC
      N=2.994E-6*(H*((TS(I)-TA)+6.2214E-4*(ES(I)-EA))+2.6853E3
      !*EVL*(TF-TA)+1.1178E-14*(TS(I)-TA))/EVL
      R(I)=10.*EVL*N
      IF(I.EQ.10)RT(I)=R(I)
      IF(I.GT.10)RT(I)=RT(I-10)+R(I)
      DC=SQRT(2.8254E-4*R(I)+DC*DC)
100   CONTINUE
      DO 200 I=60,600,60
      WRITE(6,150)I,E(I),TS(I),R(I),RT(I)
150   FORMAT(10X,I3,5X,4(E12.5,5X))
200   CONTINUE
      STOP
      END
```